

# On the Question of Stability, Conjugation, and “Aromaticity” in Imidazol-2-ylidenes and Their Silicon Analogs<sup>†</sup>

Christoph Heinemann,<sup>‡</sup> Thomas Müller,<sup>§</sup> Yitzhak Apeloig,<sup>\*,§</sup> and Helmut Schwarz<sup>\*,‡</sup>

Contribution from the Institut für Organische Chemie der Technischen Universität Berlin, Strasse des 17. Juni 135, D-10623 Berlin, Germany, and Department of Chemistry, Technion-Israel Institute of Technology, Haifa 32000, Israel

Received July 14, 1995<sup>⊗</sup>

**Abstract:** Thermodynamic, structural, and magnetic criteria, the properties of the charge distributions, and low-energy ionization processes are theoretically analyzed to learn about the role of  $\pi$ -electron delocalization in recently synthesized stable singlet carbenes (Arduengo et al. *J. Am. Chem. Soc.* **1991**, *113*, 361) and silylenes (Denk et al. *J. Am. Chem. Soc.* **1994**, *116*, 2691) of the imidazol-2-ylidene type and also in related model systems. The different approaches show consistently that cyclic electron delocalization does indeed occur in the C=C unsaturated imidazol-2-ylidene systems, in particular with respect to the corresponding C–C saturated imidazolin-2-ylidenes. However, the conclusion regarding the degree of conjugation and aromaticity depends on the criteria used, being quite small according to the “atoms-in-molecules” charge analysis but more significant according to the energetic and the magnetic properties. According to all criteria, the aromatic character of imidazol-2-ylidenes is less pronounced compared to benzene or the imidazolium cation.  $\pi$ -Electron resonance is found to be less extensive in the silylenes compared to their carbene analogs.

## Introduction

For a long time, species involving divalent carbon and silicon atoms were considered to be “elusive” in the sense that they could only be directly observed by spectroscopic techniques, either in the gas-phase<sup>1</sup> or in low-temperature matrices,<sup>2</sup> but could not be isolated in macroscopic amounts at room temperature. However, the recent syntheses of stable crystalline singlet carbenes (imidazol-2-ylidenes **1** with R = adamantyl, aryl or *tert*-butyl;<sup>3</sup> imidazolin-2-ylidenes **2** with R = aryl<sup>4</sup>) and silylenes (**3**, **4** with R = *tert*-butyl<sup>5,6</sup>) have changed our views of these species. These discoveries have stimulated research on the electronic structure of these novel divalent species and on the reasons for their unusual stability.<sup>7–15</sup>

The present study addresses the question whether the C=C-unsaturated Arduengo-type carbenes **1** (Scheme 1) and their silicon analogs **3** benefit from “aromaticity”, i.e. from cyclic  $6\pi$ -electron delocalization. A critical role of the C=C double bond in stabilizing **1** (and **3**) might have been suspected intuitively from the fact that in the carbon case the corresponding imidazolin-2-ylidenes **2**, in which the olefinic backbone of the five-membered ring is transformed into a saturated hydrocarbon moiety, had not been isolated until mid 1995<sup>4</sup> despite numerous attempts. During the 1960s, Wanzlick and co-workers showed that compounds of type **2** could be generated in solution in a very similar manner to **1**,<sup>16</sup> but in the absence of scavenger reagents they could only observe carbene dimerization products. The carbene itself was never isolated. However, very recently, actually in a paper which came to our attention when this work

<sup>†</sup> Dedicated to Prof. Chava Lifshitz, Jerusalem, on the occasion of her 60th birthday.

<sup>‡</sup> Berlin.

<sup>§</sup> Haifa.

<sup>⊗</sup> Abstract published in *Advance ACS Abstracts*, February 1, 1996.

(1) For example: (a) Leopold, D. G.; Murray, K. K.; Lineberger, W. C. *J. Chem. Phys.* **1984**, *81*, 1048. (b) Srinivas, R.; Bohme, D. K.; Schwarz, H. J. *Phys. Chem.* **1993**, *97*, 13643. (c) McGibbon, G. A.; Kingsmill, C. A.; Terlouw, J. K. *Chem. Phys. Lett.* **1994**, *222*, 129. (d) Burgers, P. C.; McGibbon, G. A.; Terlouw, J. K. *Chem. Phys. Lett.* **1994**, *224*, 539. (e) McGibbon, G. A.; Burgers, P. C.; Terlouw, J. K. *Int. J. Mass Spectrom. Ion Processes* **1994**, *136*, 191.

(2) For example: (a) Drahnak, T.; Michl, J.; West, R. *J. Am. Chem. Soc.* **1979**, *101*, 5527. (b) Maier, G.; Glatthaar, J.; Reisenauer, H. P. *Chem. Ber.* **1989**, *122*, 2403. (c) Gillette, G. R.; Noren, G.; West, R. *Organometallics* **1990**, *9*, 2925. (d) Veith, M.; Werle, E.; Lisowski, R.; Löppe, R.; Schnöckel, H. *Chem. Ber.* **1992**, *125*, 1375.

(3) (a) Arduengo, A. J., III; Harlow, R. L.; Kline, M. *J. Am. Chem. Soc.* **1991**, *113*, 361. (b) Arduengo, A. J., III; Rasika Dias, H. V.; Harlow, R. L.; Kline, M. *J. Am. Chem. Soc.* **1992**, *114*, 5530. (c) For a brief review, see: Regitz, M. *Angew. Chem.* **1991**, *103*, 691; *Angew. Chem., Int. Ed. Engl.* **1991**, *30*, 674.

(4) Arduengo, A. J., III; Goerlich, J. R.; Marshall, W. J. *J. Am. Chem. Soc.* **1995**, *117*, 11027.

(5) Denk, M.; Lennon, R.; Hayashi, R.; West, R.; Belyakov, A. V.; Verne, H. P.; Haaland, A.; Wagner, M.; Metzler, N. *J. Am. Chem. Soc.* **1994**, *116*, 2691.

(6) Denk, M.; Green, J. C.; Metzler, N.; Wagner, M. *J. Chem. Soc., Dalton Trans.* **1994**, 2405.

(7) Arduengo, A. J., III; Rasika Dias, H. V.; Dixon, D. A.; Harlow, R. L.; Klooster, W. T.; Koetzle, T. F. *J. Am. Chem. Soc.* **1994**, *116*, 6812.

(8) Arduengo, A. J., III; Dixon, D. A.; Harlow, Kumashiro, K. K.; Lee, C.; Power, W. P.; Zilm, K. W. *J. Am. Chem. Soc.* **1994**, *116*, 6361.

(9) Arduengo, A. J., III; Bock, H.; Chen, H.; Denk, M.; Dixon, D. A.; Green, J. C.; Herrmann, W. A.; Jones, N. L.; Wagner, M.; West, R. *J. Am. Chem. Soc.* **1994**, *116*, 6641.

(10) Dixon, D. A.; Arduengo, A. J., III *J. Phys. Chem.* **1991**, *95*, 4180.

(11) Cioslowski, J. *Int. J. Quantum Chem: Quantum Chem. Symp.* **1993**, *27*, 309.

(12) Heinemann, C.; Thiel, W. *Chem. Phys. Lett.* **1994**, *217*, 11.

(13) Apeloig, Y.; Karni, M.; Müller, T. In *Organosilicon Chemistry II*; VCH: Weinheim, in press.

(14) Nyulászai, L.; Kárpáti, T.; Veszprémi, T. *J. Am. Chem. Soc.* **1994**, *116*, 7239.

(15) Heinemann, C.; Herrmann, W. A.; Thiel, W. *J. Organomet. Chem.* **1994**, *475*, 73.

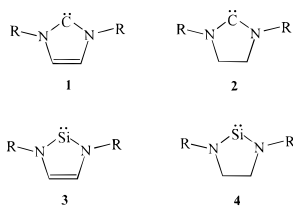
(16) (a) Wanzlick, H.-W.; Schikora, E. *Angew. Chem.* **1960**, *72*, 494.

(b) Schikora, E. Ph.D. Thesis, Technical University Berlin, D83, 1961. (c)

Wanzlick, H.-W. *Angew. Chem.* **1962**, *74*, 129. (d) Lemal, D. M.; Kawano, K. I. *J. Am. Chem. Soc.* **1962**, *84*, 1761. (e) Lemal, D. M.; Lovald, R. A.; Kawano, K. I. *J. Am. Chem. Soc.* **1964**, *86*, 2518. (f) Schönherr, H.-J. Ph.D. Thesis, Technical University Berlin, D83, 1970. Besides studies on the C–C-saturated imidazolin-2-ylidenes **2**, this work also reports efforts to synthesize the C–C-unsaturated imidazol-2-ylidenes **1**. However, upon deprotonation of 1,3-disubstituted imidazolium salts, which is basically the procedure used in refs 3a and 4, no carbenes could be isolated: (g) Schönherr, H.-J.; Wanzlick, H.-W. *Chem. Ber.* **1970**, *103*, 1037.

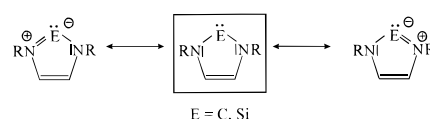
**Table 1.** Previous Studies on Imidazol-2-ylidenes and Their Silicon Analogs

property studied	method	conclusions	ref
Carbenes			
electronic structure of imidazol-2-ylidene in the lowest singlet and triplet states; proton affinity	correlated ab initio calculations	bonding character carbenic rather than ylidic; $\pi$ -delocalization important in imidazolium cation but not in the carbene	10
electronic structure of imidazol-2-ylidene: bond orders, atomic charges, localized natural orbitals	correlated ab initio calculations	stabilization of singlet ground state by $\sigma$ -back-donation along C–N bonds; $\pi$ -delocalization plays only a minor role in imidazol-2-ylidene, but a major role in imidazolium cation	11
electronic structure of aminocarbenes: singlet–triplet splittings, Mulliken populations, barriers for 1,2-rearrangements to imines	correlated ab initio calculations	singlet–triplet splitting in imidazol-2-ylidene 15 kcal/mol higher than in imidazolin-2-ylidene; consequently smaller propensity of the former towards dimerization; imidazol-2-ylidene kinetically stable toward rearrangement to imidazole	12
chemical shielding tensor of a substituted imidazol-2-ylidene	solid-state NMR; Correlated ab initio and density-functional calculations	dominance of carbenic over ylidic resonance structures in <b>1</b>	8
photoelectron spectra of <b>1</b> and <b>3</b>	Photoelectron spectroscopy; density-functional calculations	degree of interaction between the $\pi$ -electrons of the five-membered ring and the divalent group 14 atom higher in silylene <b>3</b> as compared to carbene <b>1</b>	9
electron distribution in a substituted imidazol-2-ylidene	X-ray and neutron diffraction; density-functional calculations	$\pi$ -delocalization not dominant in imidazol-2-ylidenes; stability of <b>1</b> is kinetic in origin	7
electronic structure of stable carbenes, silylenes, and germylenes	correlated ab initio calculations	$\pi$ -delocalization more extensive in <b>1</b> compared to <b>2</b> ; <b>1</b> has partial aromatic character; similar conclusions for isostructural silylenes and germylenes	19
Silylenes			
gas-phase structure and solution-phase NMR of <b>3</b> , theoretical heats of hydrogenation for <b>3</b> and <b>4</b>	electron diffraction; correlated ab initio calculations	<b>3</b> benefits from aromatic stabilization	5
photoelectron spectra of <b>3</b> and <b>4</b> ; rotational barriers in Si(NH <sub>2</sub> ) <sub>2</sub> and C(NH <sub>2</sub> ) <sub>2</sub>	photoelectron spectroscopy; correlated ab initio calculations	significant $p_\pi$ – $p_\pi$ interaction between divalent group 14 center and amino substituent; aromatic resonance structures contribute significantly in <b>3</b>	6
chemical shifts and anisotropies in aminosilylenes	correlated ab initio calculations	significant degree of $6\pi$ -aromaticity in <b>3</b>	13

**Scheme 1**

was in progress, Arduengo and co-workers made a spectacular achievement by isolating and characterizing a stable crystalline imidazolin-2-ylidene **2** which melts at 109 °C without decomposition.<sup>4</sup> Whether the C–C saturated cyclocarbenes **2** are thermodynamically less stable than their potentially aromatic C=C unsaturated counterparts is an open question to which the present report contributes from the theoretical point of view. In this context, it is worthwhile mentioning that enhanced reactivity has been observed for the isolable and isostructural silylenes **4** (relative to **3**) and germylenes, and this was interpreted as due to missing aromatic stabilization.<sup>15,17</sup>

In a number of experimental<sup>6–9</sup> and theoretical studies<sup>10–15</sup> the electronic structures of imidazol-2-ylidenes, imidazolin-2-ylidenes, and their silicon and germanium analogs have already been investigated. The major conclusions of these works are summarized in Table 1. Most of the available data on imidazol-

**Scheme 2**

2-ylidenes **1** point to a true carbene with only negligible importance of  $\pi$ -delocalized ylidic resonance structures (Scheme 2).<sup>8,10,11</sup> On the other hand, there is also agreement in the literature that the isostructural silylenes **3** do in fact benefit from aromatic  $6\pi$ -electron delocalization.<sup>5,6,13,14</sup> Si–N  $\pi$ -bonding and linear conjugation, a prerequisite for cyclic electron delocalization in cyclosilylenes, have been deduced from the high and nonadditive rotational barriers in diaminosilylene.<sup>6</sup> Recent measurements of the photoelectron spectra of **1** and **3** have revealed that there appears to be a higher out-of-plane electron density at the divalent center in **3** as compared to **1**.<sup>9</sup> To explain this counterintuitive result, the authors suggested contributions from a valene-bond structure involving a neutral silicon atom chelated by 1,4-diazabutadiene.<sup>9</sup> The relation of this interesting concept to the idea of cyclic electron delocalization or direct  $p_\pi$ – $p_\pi$  resonance remains to be investigated. In any case, it would be surprising if the resonance stabilization in **3** would be more extensive than in **1** in light of the commonly accepted view that  $p_\pi$ – $p_\pi$  bonds involving silicon are intrinsically weaker compared to their carbon analogs.<sup>18</sup> As it was concluded that  $\pi$ -delocalization is of only minor importance in the C=C unsaturated carbenes **1**, chemical differences relative to their C–C saturated counterparts **2** cannot be due to the specific

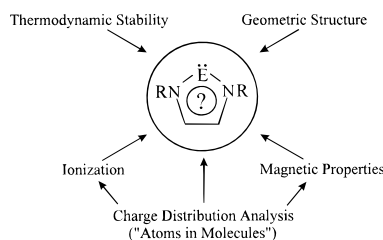
(17) Herrmann, W. A.; Denk, M.; Behm, J.; Scherer, W.; Klingan, F. R.; Bock, H.; Solouki, B.; Wagner, M. *Angew. Chem.* **1992**, *104*, 1489; *Angew. Chem., Int. Ed. Engl.* **1992**, *31*, 1485.

electronic situation at the carbene center and they were therefore explained in terms of kinetic barriers associated with electrostatic repulsion between the localized  $\pi$ -electrons of the C=C double bond and a potential nucleophilic reaction partner.<sup>7</sup> On the other hand, the calculated excitation energy from the singlet ground state to the lowest triplet state increases by 15 kcal/mol in going from imidazolin-2-ylidene (**2** with R = H) to imidazol-2-ylidene (**1** with R = H), indicating significant differences in the electronic structures of these two molecules.<sup>12</sup> Note, however, that the overall singlet–triplet splittings are in the range of 65–85 kcal/mol, thus clearly indicating a large stabilization of both **1** and **2** with respect to the triplet ground state methylene, CH<sub>2</sub>. After this study had been completed we learned from a related theoretical investigation by Böhme and Frenking<sup>19</sup> who have also studied the thermodynamic, structural, and magnetic properties of the above-mentioned stable cyclocarbenes and their higher homologs arriving at the conclusion, that the presence of the C=C double bond in the five-membered rings brings about enhanced  $p_{\pi}$ – $p_{\pi}$  “aromatic” delocalization.

In view of the above introduction and the data collected in Table 1, it seems that a consistent answer to the question to which extent cyclic electron delocalization stabilizes the electronic structure of the Arduengo-type carbenes **1** and their higher homologs still needs to be given. A sceptical objection to this inquiry is that the topic is mostly semantic.<sup>10,12</sup> However, a very different viewpoint can be advocated as well: “aromaticity”<sup>20</sup> remains one of the most useful concepts in chemistry and arguments linking  $\pi$ -conjugation with kinetic or thermodynamic stability are widely used in the literature. In order to attempt to reach a conclusion as balanced and nonbiased as possible we apply three common criteria to establish whether molecules such as **1** and **3** have significant aromatic character. The criteria are thermodynamic stability, geometric structure, and magnetic properties. As an additional approach to understanding the properties of the molecular charge distributions with regard to the question of electron delocalization, we employ the theory of “atoms-in-molecules” as developed by Bader and co-workers.<sup>21,22</sup> Also the two lowest ionization processes<sup>9</sup> of model systems for **1** and **3** (R = H) will be analyzed with regard to  $\pi$ -electron delocalization. To provide a link between the different approaches, Bader’s theory will be employed not only for charge distribution analysis in the neutral carbenes and silylenes but also for studying the atomic contributions to their magnetic properties as well as the electronic structures of the radical cations which arise upon ionization. Our approach is graphically summarized in Scheme 3.

Since the problem at hand does not allow for a simple binary decision (“aromatic or not?”), our final answer will be more qualitative in nature. However, we hope that a careful comparison of several aromaticity criteria will provide deeper insight into the fascinating chemistry of stable carbenes,<sup>23,24</sup> silylenes, and other isoelectronic analogs.<sup>25</sup> The present investigation does not cover recently characterized stable triplet

### Scheme 3



carbenes<sup>26</sup> and a class of carbon-, phosphorus-, and silicon-containing molecules synthesized by Bertrand and co-workers,<sup>27</sup> for which carbenic character has been discussed but ultimately disproved on the basis of theoretical analyses.<sup>28</sup>

### Theoretical Methods

Energies for thermodynamic comparisons were obtained using complete fourth-order Møller–Plesset (MP4; frozen core approximation, fc) single-point calculations at geometries optimized with the Hartree–Fock (HF) method and the 6-31G(d) basis set.<sup>29</sup> The respective minima were positively identified by 3N – 6 positive eigenvalues of their force-constant matrices and the HF/6-31G(d) zero-point vibrational energies (ZPVE) were added to the MP4 energies to obtain the final reaction energies (MP4SDTQ(fc)/6-31G(d)/HF/6-31G(d) + ZPVE). In the calculations of rotational barriers and ionization energies, electron correlation was treated by second- to fourth-order Møller–Plesset perturbation theory (MPn, n = 2–4) and by the coupled-cluster

(23) For main-group and transition-metal complexes as well as other new compounds deriving from imidazol-2-ylidene, see, e.g.: (a) Wanzlick, H.-W.; Schönherr, H.-J. *Angew. Chem., Int. Ed. Engl.* **1968**, *7*, 141. (b) Öfele, K. *J. Organomet. Chem.* **1968**, *12*, P42. (c) Luger, V. P.; Ruban, G. *Acta Crystallogr.* **1971**, *B27*, 2276. (d) Arduengo, A. J. III; Kline, M.; Calabrese, J. C.; Davidson, F. J. *J. Am. Chem. Soc.* **1991**, *113*, 9704. (e) Bonati, F.; Burini, A.; Pietroni, B. R.; Bovio, B. *J. Organomet. Chem.* **1991**, *408*, 271. (f) Arduengo, A. J. III; Dias, H. V. R.; Calabrese, J. C.; Davidson, F. *J. Am. Chem. Soc.* **1992**, *114*, 9724. (g) Fehlhammer, W. P.; Bliss, P.; Fuchs, J.; Holzmann, G. *Z. Naturforsch. B., Chem. Sci.* **1992**, *47*, 79. (h) Arduengo, A. J. III; Dias, H. V. R.; Calabrese, J. C.; Davidson, F. *Inorg. Chem.* **1993**, *32*, 1541. (i) Arduengo, A. J. III; Dias, H. V. R.; Davidson, F.; Harlow, R. L. *J. Organomet. Chem.* **1993**, *462*, 13. (j) Arduengo, A. J. III; Dias, H. V. R.; Calabrese, J. C.; Davidson, F.; *Organometallics* **1993**, *12*, 34505. (k) Öfele, K.; Herrmann, W. A.; Mihalios, D.; Elison, M.; Herdtweck, E.; Scherer, W.; Mink, J. *J. Organomet. Chem.* **1993**, *459*, 177. (l) Kuhn, N.; Kratz, T.; Henkel, G. *J. Chem. Soc., Chem. Commun.* **1993**, 1778. (m) Arduengo, A. J., III; Gamper, S. F.; Calabrese, J. C.; Davidson, F. *J. Am. Chem. Soc.* **1994**, *116*, 4391. (n) Arduengo, A. J., III; Tamm, M.; Calabrese, J. C. *J. Am. Chem. Soc.* **1994**, *116*, 3625. (o) Kuhn, N.; Henkel, G.; Kratz, T. *Chem. Ber.* **1993**, *126*, 2047. (p) Arduengo, A. J. III; Tamm, M.; McLain, S. J.; Calabrese, J. C.; Davidson, F.; Marshall, W. J. *J. Am. Chem. Soc.* **1994**, *116*, 7927. (q) Schumann, H.; Glanz, M.; Winterfeld, J.; Hemling, H.; Kuhn, N.; Kratz, T. *Angew. Chem., Int. Ed. Engl.* **1994**, *33*, 1733. (r) Arduengo, A. J. III; Gamper, S. F.; Tamm, M.; Calabrese, J. C.; Davidson, F.; Craig, H. A. *J. Am. Chem. Soc.* **1995**, *117*, 572. (s) Schäfer, A.; Weidenbruch, M.; Saak, W.; Pohl, S. *J. Chem. Soc., Chem. Commun.* **1995**, 1157. (t) Kuhn, N.; Kratz, T.; Bläser, D.; Boese, R. *Chem. Ber.* **1995**, *128*, 245. (u) Alder, R. W.; Allen, P. R.; Williams, S. J. *J. Chem. Soc., Chem. Commun.* **1995**, 1267.

(24) Recently, a new stable carbene based on the 4,5-dihydro-1H-1,2,4-triazol-5-ylidene ring system has been synthesized: Enders, D.; Breuer, K.; Raabe, G.; Runsink, J.; Teles, J. H.; Melder, J.-P.; Ebel, K.; Brode, S. *Angew. Chem.* **1995**, *107*, 1119; *Angew. Chem., Int. Ed. Engl.* **1995**, *34*, 1012.

(25) Brown, D. S.; Decken, A.; Cowley, A. H. *J. Am. Chem. Soc.* **1995**, *117*, 5421.

(26) Tomioka, H.; Watanabe, T.; Hirai, K.; Furukawa, K.; Takui, T.; Itoh, K. *J. Am. Chem. Soc.* **1995**, *117*, 6376.

(27) (a) Igau, A.; Grützmaier, H.; Baccaredo, A.; Bertrand, G. *J. Am. Chem. Soc.* **1988**, *110*, 6463. (b) Igau, A.; Baccaredo, A.; Trinquier, G.; Bertrand, G. *Angew. Chem.* **1989**, *101*, 617; *Angew. Chem., Int. Ed. Engl.* **1989**, *28*, 621. (c) Gillette, G.; Igau, A.; Alcaraz, G.; Wecker, U.; Baccaredo, A.; Dahan, F.; Bertrand, G. *Angew. Chem.* **1995**, *107*, 1358.

(28) (a) Dixon, D. A.; Dobbs, K. D.; Arduengo, A. J., III; Bertrand, G. *J. Am. Chem. Soc.* **1991**, *113*, 8782. (b) Soleilhavoup, M.; Baccaredo, A.; Treutler, O.; Ahlrichs, R.; Nieger, M.; Bertrand, G. *J. Am. Chem. Soc.* **1992**, *114*, 10959. (c) Treutler, O.; Ahlrichs, R.; Soleilhavoup, M. *J. Am. Chem. Soc.* **1993**, *115*, 8788.

(18) (a) Schmidt, M. W.; Truong, P. N.; Gordon, M. S. *J. Am. Chem. Soc.* **1987**, *109*, 5217. (b) Raabe, G.; Michl, J. In *The Chemistry of Organic Silicon Compounds*; Patai, S., Rappoport, Z., Eds.; Wiley: New York, 1989. (c) Apeloig, Y. In *The Chemistry of Organic Silicon Compounds*; Patai, S., Rappoport, Z., Eds.; Wiley: New York, 1989. (d) Karni, M.; Apeloig, Y. *J. Am. Chem. Soc.* **1990**, *112*, 8589.

(19) Böhme, C.; Frenking, G. *J. Am. Chem. Soc.* **1996**, *118*, 2039–2046.

(20) For a recent monograph on this topic, see: Minkin, V. I.; Glukhovtsev, M. N.; Simkin, B. Y. *Aromaticity and Antiaromaticity*; J. Wiley & Sons: New York, 1994.

(21) Bader, R. F. W. *Atoms in Molecules - A Quantum Theory*; Oxford University Press: Oxford, 1990.

(22) For a recent application of this theory to the issue of resonance in the allyl cation, neutral, and anion, see: Gobbi, A.; Frenking, G. *J. Am. Chem. Soc.* **1994**, *116*, 9275, 9287.

approach including single and double excitations and/or a perturbational estimate of the triple contributions (CCSD(T)).<sup>30</sup> In open-shell systems Schlegel's spin-projection method<sup>31</sup> was employed to eliminate spurious high-spin contributions in the MP $n$  calculations based on unrestricted Hartree–Fock reference functions.

The discussion of structural criteria for electron delocalization refers to MP2(fc)/6-31G(d) geometries. The analyses of molecular charge distributions are based on Hartree–Fock wave functions computed within the 6-311G(d,p) basis set at the HF/6-31G(d) equilibrium geometries. The use of single-determinant wave functions for the description of singlet carbenes, which is clearly not appropriate from an energetic point of view, has been justified for charge distribution analysis in an earlier investigation by MacDougall and Bader<sup>32</sup> and is valid in the present case because of the large singlet–triplet splittings in both aminocarbenes and -silylenes.<sup>10,12</sup> All geometry optimizations and energy calculations employed the GAUSSIAN92 program.<sup>29a</sup> Magnetic susceptibility calculations were performed with Kutzelnigg's IGLO program<sup>33</sup> using basis set II<sup>33</sup> and MP2(fc)/6-31G(d) optimized geometries.

The theory of “atoms-in-molecules” has been reviewed in the literature<sup>34</sup> and in a recent monograph.<sup>21</sup> For the convenience of the reader, we will summarize some important points here. The topological characteristics of the total charge density  $\rho(\mathbf{r})$  give rise to a rigorous partitioning of the real space comprising a molecule into different atomic basins. Properties like charges, dipole, and quadrupole moments can thus unequivocally be assigned to individual atoms by integration of the desired property over their atomic basins. Chemical bonds between pairs of atoms can be identified by (3,–1) critical points (also called “bond critical points”) of the charge density  $\rho(\mathbf{r})$ . At such points  $\mathbf{r}_b$  the gradient vector of  $\rho(\mathbf{r})$  vanishes. The notation (3,–1) implies that, in addition, the Hessian matrix of  $\rho(\mathbf{r})$  at  $\mathbf{r}_b$  has three nonvanishing eigenvalues  $\lambda_1$ ,  $\lambda_2$ , and  $\lambda_3$ , two of which (usually those denoted  $\lambda_1$  and  $\lambda_2$ ) are negative. The corresponding eigenvectors belong to trajectories in real space along which  $\rho(\mathbf{r})$  is at a local maximum at  $\mathbf{r}_b$  (paths orthogonal to the actual bond path), whereas the positive eigenvalue ( $\lambda_3$ ) is associated with the bond path itself along which the charge density reaches a minimum at  $\mathbf{r}_b$ . The charge density at the bond critical point,  $\rho(\mathbf{r}_b)$ , provides a measure for the covalent bond order between a given pair of atoms. Furthermore, the value of the Laplacian of  $\rho(\mathbf{r})$  at the bond critical point,  $\nabla^2\rho(\mathbf{r}_b)$ , i.e. the sum of the three eigenvalues  $\lambda_1$ ,  $\lambda_2$ , and  $\lambda_3$ , indicates whether covalent or ionic interactions prevail between the two bonded atoms: In the former case,  $\nabla^2\rho(\mathbf{r}_b)$  tends to negative values, since aggregation of charge along the trajectories orthogonal to the actual bond path dominates over charge concentration in the atomic basins. The more ionic an interaction becomes the more localized become the charge concentrations on the atoms themselves, thus the third positive eigenvalue  $\lambda_3$  becomes larger and the value of the Laplacian is more positive. The ratio between the two negative eigenvalues  $\lambda_1$  and  $\lambda_2$  reveals whether charge concentration along a given bond occurs preferentially in a certain direction.<sup>35</sup> This allows to identify  $\pi$ -type interactions between two atoms without referring to the concept of atomic orbitals: For example, in ethane the two negative curvatures of the total charge density at the bond critical point have the same value. In ethylene the charge density falls off from the bond

critical point less rapidly in the  $\pi$ -plane as compared to the plane of the nuclei. The axis of the less negative curvature  $\lambda_2$  is called the “major” axis of the bond. For a quantitative assessment of such effects one defines the bond ellipticity  $\epsilon = [(\lambda_1/\lambda_2) - 1]$ . A set of typical  $\epsilon$ -values for several representative C–C bonds is 0.00 (ethane) 0.23 (benzene) and 0.45 (ethylene),<sup>35</sup> indicating the different degree of  $\pi$ -bonding in these molecules.<sup>36</sup> Finally, an analysis of valence shell charge concentrations<sup>37</sup> (VSCCs) will be of interest for the present purpose: Parts of the valence shell of an atom where charge is locally concentrated are identified by the presence of (3,–3) critical points<sup>38</sup> of the negative of the Laplacian of  $\rho(\mathbf{r})$ ,  $-\nabla^2\rho(\mathbf{r})$ . At such points, the charge density is higher compared to an average taken over the values found in the direct neighborhood. Moreover, one can classify a maximum in the VSCC as “bonded”, if it corresponds to a local charge concentration along a bond path, or “nonbonded”, if it is not associated with a particular atomic interaction. For example, the VSCC of the nitrogen atom in ammonia exhibits three bonded and one nonbonded maxima, respectively. For the determination of critical points in the charge density, atomic properties in molecules and critical points in the Laplacian of the charge distribution the PROAIMV package (rev. B)<sup>39</sup> was employed. The calculations of magnetic susceptibilities and their analysis in terms of atomic contributions were performed at McMaster University according to procedures described recently.<sup>40</sup> Here, the MP2/6-31G(d) optimized geometries were employed and the susceptibility calculations (using the IGAIM method<sup>41</sup>) used the 6-31G(d,p) basis set.

## Results and Discussion

The paper is organized as follows: First we will discuss the thermodynamic, structural and magnetic criteria for electron delocalization. The following section then deals with the analysis of the properties of the total charge distributions by help of the theory of “atoms-in-molecules”. Lastly, the low-energy ionization processes are investigated. A comparison of the results obtained with the different approaches and our conclusions with respect to the degree of electron delocalization in the investigated stable carbenes and silylenes will be given in a final section.

**I. Thermodynamic Criteria.** At the outset, let us first remind the reader that the conducted quantum-chemical study treats isolated molecules unaffected by bulk and environment effects; in this context “stability” has a strictly *thermodynamic* meaning and does not necessarily cover all aspects of chemical stability. High thermodynamic stability may imply also *kinetic* stability and thus low reactivity, but this is not necessarily the case. Another point which we would like to stress is that there is no direct way to correlate the degree of conjugation with the resulting thermodynamic stabilization.<sup>20</sup>

To estimate the thermodynamic stabilization energies of various aminocarbenes and -silylenes with respect to the parent singlet species  ${}^1\text{CH}_2$  and  ${}^1\text{SiH}_2$ , respectively, we consider a systematic series of isodesmic reactions (a–e), as defined in Scheme 4. The calculated reaction energies are summarized in Table 2. Let us first examine what can be learned from

(29) (a) Gaussian 92/DFT, Revision F.2, Frisch, M. J.; Trucks, G. W.; Schlegel, H. W.; Gill, P. M. W.; Johnson, B. G.; Wong, M. W.; Foresman, J. B.; Robb, M. A.; Head-Gordon, M.; Replogle, E. S.; Gomperts, R.; Andres, J. L.; Raghavachari, K.; Binkley, J. S.; Gonzales, C.; Martin, R. L.; Fox, D. J.; Defrees, D. J.; Baker, J.; Stewart, J. J. P.; Pople, J. A., Gaussian, Inc., Pittsburgh, PA, 1993. (b) Hehre, W. J.; Radom, L.; Schleyer, P. v. R.; Pople, J. A. *Ab initio Molecular Orbital Theory*; Wiley: New York, 1986.

(30) Pople, J. A.; Head-Gordon, M.; Raghavachari, K. *J. Chem. Phys.* **1987**, *87*, 5968.

(31) (a) Schlegel, H. B. *J. Chem. Phys.* **1986**, *84*, 4530. (b) Schlegel, H. B. *J. Phys. Chem.* **1988**, *92*, 3075.

(32) MacDougall, P. J.; Bader, R. F. W. *Can. J. Chem.* **1986**, *64*, 1496.

(33) For a recent review, see: Kutzelnigg, W.; Fleischer, U.; Schindler, M. *NMR Basic Princ. Prog.* **1991**, *23*, 165.

(34) (a) Bader, R. F. W. *Acc. Chem. Res.* **1975**, *8*, 34. (b) Bader, R. F. W. *Chem. Rev.* **1991**, *91*, 893. (c) Bader, R. F. W.; Popelier, P. A. L.; Keith, T. A. *Angew. Chem.* **1994**, *106*, 647; *Angew. Chem., Int. Ed. Engl.* **1994**, *33*, 620.

(35) Bader, R. F. W.; Slee, T. S.; Cremer, D.; Kraka, E. *J. Am. Chem. Soc.* **1983**, *105*, 5061.

(36) In the five-membered heterocycles of the type  $\text{X}(\text{CH}=\text{CH})_2$  the C=C bond ellipticities are 0.31, 0.37, 0.39, and 0.44 for  $\text{X}=\text{CH}^-$ , S, NH, and O, respectively, in agreement with their commonly accepted degrees of aromaticity, see: (a) Schleyer, P. v. R.; Freeman, P. K.; Jiao, H.; Goldfuss, B. *Angew. Chem.* **1995**, *107*, 332; *Angew. Chem., Int. Ed. Engl.* **1995**, *34*, 337. (b) Goldfuss, B.; Schleyer, P. v. R. *Organometallics* **1995**, *14*, 1553. In addition, the X–C bonds have their major axes perpendicular to the molecular planes, as typical for bonds with significant  $\pi$ -contributions.

(37) Bader, R. F. W.; MacDougall, P. J.; Lau, C. D. H. *J. Am. Chem. Soc.* **1984**, *106*, 1594.

(38) This notation denotes a point with three nonvanishing and negative eigenvalues of  $\nabla^2r(\mathbf{r})$ .

(39) Biegler-König, F. W.; Bader, R. F. W.; Tang, T.-H. *J. Comput. Chem.* **1982**, *3*, 317.

(40) (a) Keith, T. A.; Bader, R. F. W. *J. Chem. Phys.* **1993**, *99*, 3669. (b) Bader, R. F. W.; Keith, T. A. *J. Chem. Phys.* **1993**, *99*, 3683.

(41) Keith, T. A.; Bader, R. F. W. *Chem. Phys. Lett.* **1992**, *193*, 1.

## Scheme 4

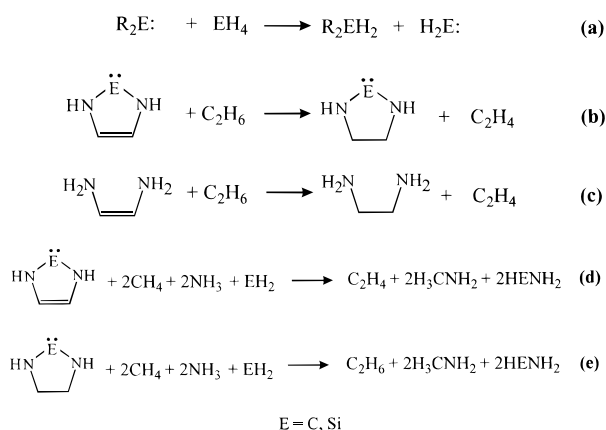


**Table 2.** Calculated Energy Changes (kcal/mol) for Isodesmic Reactions a–e (See Scheme 4)

reaction <sup>a</sup>	substitution pattern	MP4/6-31G(d)// HF/6-31G(d) + ZPVE
a1	E = C, R = NH <sub>2</sub> , perpendicular <sup>b</sup>	19.8
a2	E = C, R = NH <sub>2</sub> , planar <sup>b</sup>	86.6
a3	E = C, R = HNCH <sub>2</sub>	92.7
a4	E = C, R = HNCH=	112.1
a5	E = Si, R = NH <sub>2</sub> , perpendicular <sup>b</sup>	-5.8
a6	E = Si, R = NH <sub>2</sub> , planar <sup>b</sup>	30.0
a7	E = Si, R = HNCH <sub>2</sub>	38.7
a8	E = Si, R = HNCH=	50.5
b1	E = C	24.2
b2	E = Si	25.0
c		1.4 <sup>c</sup>
d1	E = C	1.6
d2	E = Si	30.2
e1	E = C	-22.7
e2	E = Si	5.5

<sup>a</sup> Letters refer to Scheme 4, and numbers are given for the different substitution patterns. <sup>b</sup> “Perpendicular” denotes the lowest-energy  $C_{2v}$  conformation with the two nitrogen lone pairs coplanar to the carbene lone-pair and “planar” denotes the  $C_{2v}$  minimum conformation. <sup>c</sup> Employing the lowest-energy  $C_{2v}$  structure for 1,2-diaminoethene. Relaxation of its geometry to the  $C_1$  minimum structure increases the energy of reaction c by 11.7 kcal/mol.

reactions a. Even when conjugation between the divalent carbene center and the two adjacent amino groups is not possible due to a perpendicular orientation of the nitrogen lone pairs and the “empty” carbene orbital, diaminocarbene is stabilized by ca. 20 kcal/mol with respect to singlet methylene (reaction a1). A reasonable explanation for this stabilization is the higher electronegativity of the nitrogen substituent, which effectively removes excess  $\sigma$ -electron density from the divalent carbon atom as compared to singlet  $CH_2$ .<sup>32</sup> In the planar conformation (reaction a2), this stabilization is almost 70 kcal/mol higher. The addition of a  $CH_2CH_2$  bridge between the two amino groups leads to a slight increase in the stabilization energy (+6 kcal/mol, reaction a3), whereas the unsaturated  $CH=CH$  linkage (reaction a4) has a more pronounced effect of +26 kcal/mol relative to reaction a2. The small difference between planar diaminocarbene and the C–C saturated cyclocarbene might well be due to small geometric changes at the N–C–N linkage and differences in the donor-ability of the substituted vs nonsubstituted amino groups. The traditional interpretation would relate the large difference between reactions a1 and a2 and the associated thermodynamic stabilization of planar diaminocarbene relative to the perpendicular conformation to  $p_\pi$ – $p_\pi$  delocalization. Similarly, the extra stabilization of the C=C unsaturated cyclocarbene with respect to the C–C saturated counterpart can be understood as indicating cyclic electron

delocalization in the former molecule. However, this interpretation relies on the *a priori* assumption that the  $\pi$ -electrons do in fact undergo cyclic delocalization and that such electron delocalization indeed results in thermodynamic stabilization. Since the calculated reaction energies *alone* do not provide direct insight into the charge distributions of the involved diaminocarbenes, the electronic nature of the interaction between the carbene center and an amino substituent will be analyzed in detail further below.

The energetic situation is somewhat different in the silylene series. Singlet silylene  $SiH_2$  is slightly destabilized (–6 kcal/mol) upon substitution with two perpendicularly oriented amino groups (reaction a5). In light of our explanation for the energy balance of reaction a1 (see above), this marginal *destabilization* can be rationalized by the lower electronegativity of silicon as compared to carbon, such that withdrawal of excess electron density from the divalent silicon center in the singlet state is energetically more favorable for the hydrogen compared to the nitrogen atom, which as already a fairly large electronegativity difference with respect to silicon.<sup>32</sup> Upon rotation to the planar structure (reaction a6) the molecule is stabilized by 36 kcal/mol, which is about half of the effect calculated for the isostructural carbenes (reaction a2). The extra stabilization of the C–C saturated cyclosilylene (reaction a7) with respect to the noncyclic planar diaminosilylene is again smaller (9 kcal/mol) as compared to the C=C unsaturated silylene (20 kcal/mol extra stabilization, reaction a8). If one argues that the energies of the isodesmic reactions discussed above reflect different degrees of electron delocalization, then the comparison between the silylenes and the carbenes is consistent with the general consensus that  $\pi$ -bonds between silicon and nitrogen are intrinsically weaker than  $\pi$ -bonds between carbon and nitrogen.<sup>18,42</sup>

Is the high thermodynamic stability of the C=C unsaturated carbene and silylene connected with its cyclic nature? Does the same stabilization exist also in analogous conjugated but noncyclic molecules? For both the carbene and the silylene case reaction b is highly endothermic indicating that these molecules are stabilized by the endocyclic double bond. This stabilization is not due to localized conjugative interactions in the  $HNCH=CHNH$  “backbone” of these molecules since 1,2-diaminoethene in the planar  $C_{2v}$  geometry is stabilized by only 1.4 kcal/mol with respect to 1,2-diaminoethane (reaction c).<sup>43</sup>

Bond separation processes, such as reactions d and e in which all formal bonds between non-hydrogen atoms in the cyclocarbenes and -silylenes have been separated to form the simplest two heavy-atom molecules containing bonds of the same types, are also frequently used for evaluating stabilization by conjugative interaction. Here, the absolute energy changes are only of minor interest. The important point is that for both the carbenes and the silylenes bond separation of the C=C unsaturated molecule is at least 20 kcal/mol more endothermic than for the corresponding C–C-saturated one. This is yet another energetic indication for a stabilization of the imidazol-2-ylidenes and their silicon analogs by a cooperative mechanism involving the C=C double bond, the nitrogen lone pairs and the dicoordinated central atom.

**II. Structural Criteria.** Here, we will discuss trends in the

(42) Schleyer, P. v. R.; Stout, P. D. *J. Chem. Soc., Chem. Commun.* **1986**, 1373.

(43) While the lowest energy  $C_{2v}$  structure of 1,2-diaminoethene is a third-order saddle point on the potential energy surface, we use it as the proper comparison for the “backbone” effect of the imidazol-2-ylidene ring. The  $C_1$  minimum structure is ca. 10 kcal/mol more stable (footnote c to Table 2) than the  $C_{2v}$  structure, but it is still by more than 10 kcal/mol less stabilized compared to the C=C unsaturated cyclocarbene and cyclosilylene (reactions b).

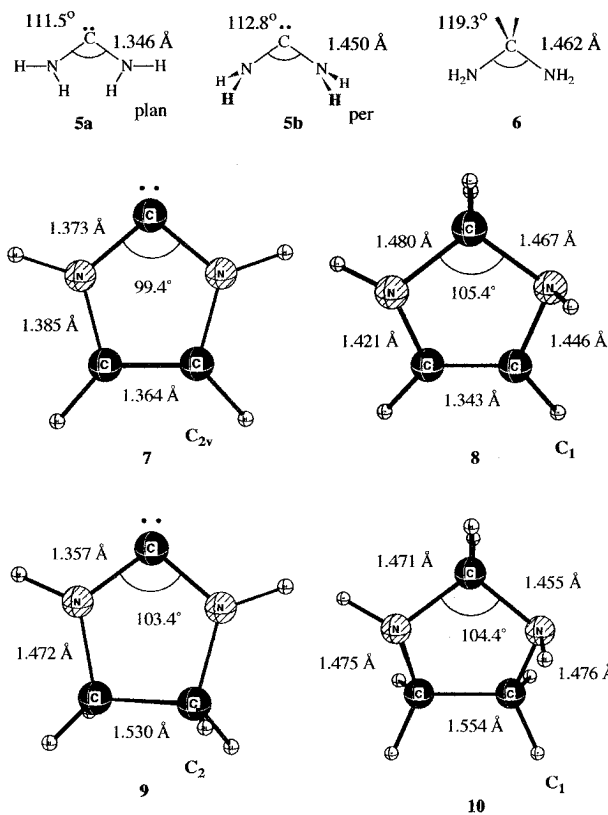


**Figure 1.** Optimized MP2/6-31G(d) geometries for model carbenes and the corresponding saturated hydrocarbons.

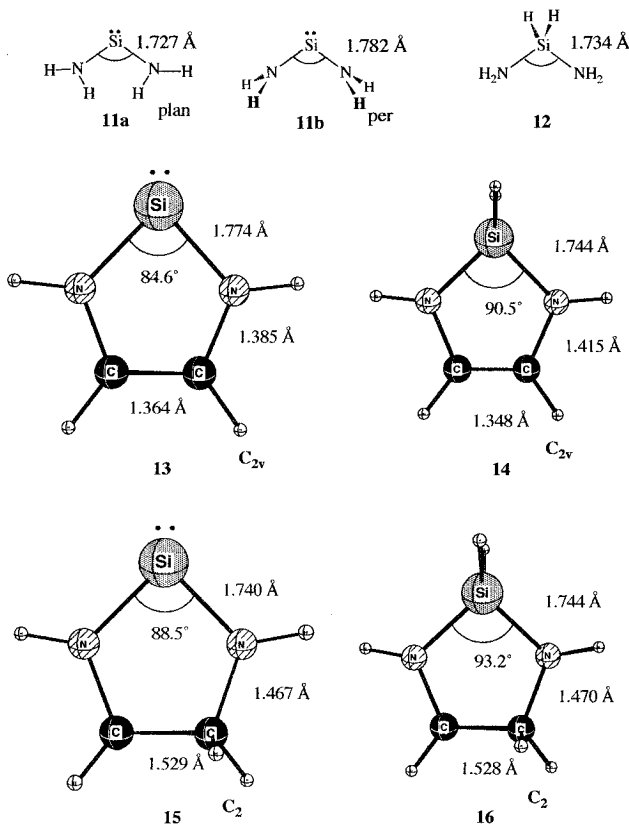


**Figure 2.** Optimized MP2/6-31G(d) geometries for model silylenes and the corresponding saturated silanes.

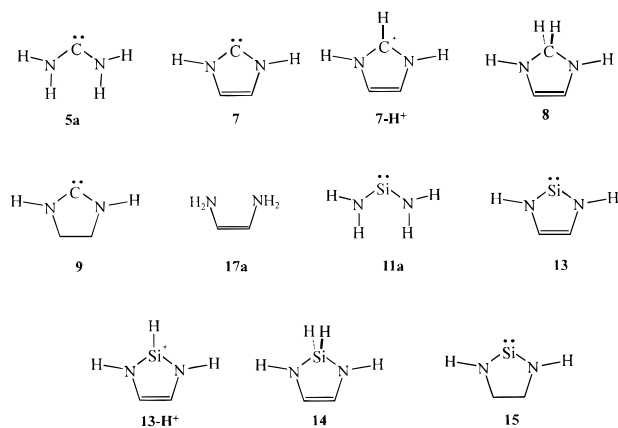
calculated geometries (MP2/6-31G(d)) of a series of model systems (see Figures 1 and 2). First, let us consider diaminocarbene **5**. In the perpendicular conformation **5b**, the C–N bond lengths are almost identical to those in diaminomethane **6**. However, these bonds shorten by 0.104 Å upon rotation of

the amino groups to the planar minimum conformation **5a**. This bond shortening can be attributed to allyl anion type<sup>22</sup>  $4\pi$ -electron delocalization along the N–C–N linkage. Now consider the cyclic systems. The carbenic carbon–nitrogen bond distance in imidazol-2-ylidene **7** is 0.103 Å shorter than the average in imidazol-2-ine **8**, which is consistent with  $p\pi$ – $p\pi$  interaction along the N–C–N moiety. Moreover, in **7** the C=C double bond is 0.021 Å longer and the average N–C distance within the N–C=C–N framework is 0.049 Å shorter compared to **8**. However, the C–C single bond in the C–C-saturated carbene imidazolin-2-ylidene (**9**) is shorter (by 0.024 Å) than in the corresponding hydrogenated imidazolidine **10**. The carbene center–nitrogen atom distance in **9** is quite similar to **5a** and 0.016 Å shorter compared to the C=C unsaturated carbene **7**. If one assumes that localized  $\pi$ -electron conjugation occurs within the N–C=C–N framework of **8** and the N–C–N moiety of **9**, these trends can consistently be interpreted as arising from bond length compensation due to cyclic electron delocalization in the C=C unsaturated imidazol-2-ylidene **7**. The calculated MP2(fc)/6-31G(d) structures for **7** and **9** agree qualitatively (trends in the bond lengths and angles discussed above) with experimental X-ray structures for the isostructural compounds **1** and **2** with R = mesityl,<sup>4</sup> and also the quantitative agreement is reasonable (maximum deviations: 0.03 Å and 2°, respectively). Arduengo and co-workers also consider the possibility that increased  $\pi$ -interactions account for the change in the carbenic carbon–nitrogen atom distances, noting, however that the small effects (0.019 Å in the experimental structures, 0.020 Å in the model systems discussed here) might also be due to  $\sigma$ -effects from associated changes in the N–C–N angle.<sup>4</sup>

Similar but smaller geometry effects are found in the isostructural cyclosilylenes and related model species shown in Figure 2. The Si–N bond lengths in the planar (**11a**) and perpendicular (**11b**) conformations of diaminosilylene differ by 0.055 Å, a change which is only ca. 50% than between the two conformers of diaminocarbene (see above). Also the C=C bond lengthening in the unsaturated cyclosilylene **13** (+0.016 Å with respect to the corresponding cyclosilane **14**) and the concomitant shortening of the N–C bond in the N–C=C–N “backbone” (–0.030 Å) are less pronounced than for the isostructural carbon species. Note, however, that the calculated Si–N bond lengths in the diaminosilanes **12**, **14**, and **16** are quite similar to those in the corresponding silylenes **11a**, **13**, and **15**. The smaller geometrical changes in the silylenes relative to the carbenes might be associated with a smaller degree of electron delocalization in the silylenes, but they might also derive from entirely different factors, such as different charge accumulations due to the lower electronegativity of silicon as compared to carbon. To conclude the discussion of the first two criteria, much of the thermodynamic and structural data discussed above are consistent with the operation of cyclic delocalization. However, this is not the only possible interpretation, and therefore it is important to supplement the structural and energetic evidence by an examination of additional independent criteria.

**III. Magnetic Criteria and Their Analysis in Terms of Atomic Contributions.** A significant anisotropy of the magnetic susceptibility  $\Delta\chi$  is regarded as an indication for a ring current and thus of cyclic electron delocalization and aromaticity.<sup>20</sup> For a recent discussion of this issue within the framework of the “atoms-in-molecules” theory, the reader is referred to the literature.<sup>40</sup> We consider first some magnetic properties and their atomic contributions for imidazol-2-ylidene **7**, imidazolin-2-ylidene **9**, and the imidazolium cation **7-H**<sup>+</sup>. Later, calculated  $\Delta\chi$  values will be analyzed for the larger set

## Scheme 5



of model systems shown in Scheme 5. The numerical results are given in Tables 3 and 4.

As evident from the results shown in Table 3, the major contributions to the magnetic susceptibilities and their anisotropies in **7**, **7-H<sup>+</sup>**, and **9** are due to the atoms in the five-membered ring. The absolute average magnetic susceptibilities are quite similar for all three molecules. However, both **7** ( $\Delta\chi = -7.84$  au) and **7-H<sup>+</sup>** ( $\Delta\chi = -7.64$  au) have significantly larger anisotropies  $\Delta\chi$  than the C–C-saturated cyclic carbene **9** ( $\Delta\chi = -3.25$  au). Inspection of the atomic contributions reveals that for the C=C unsaturated molecules more than 80% (**7**, 81%; **7-H<sup>+</sup>**, 84%) of  $\Delta\chi$  are due to  $\Delta\chi_f$  contributions from ring atoms, i.e. to fluxes of the magnetically induced current through interatomic surfaces of the ring atoms. The induced currents through the interatomic surfaces are larger when the magnetic field is applied perpendicular to the molecular plane, which is typical for a delocalized  $\pi$ -type electron distribution, as found in benzene.<sup>40</sup> For comparison,  $\Delta\chi$  for benzene (calculated with the same method and basis set) is  $-13.83$  au and the fluxes through the C–C surfaces contribute 85%.<sup>44</sup>

A second indication for ring currents in both **7** and **7-H<sup>+</sup>** are the atomic contributions to the shielding tensors<sup>45</sup> (i.e. the integral of the shielding density  $\mathbf{r}_N \times \mathbf{J}^{(1)}(\mathbf{r})/\mathbf{r}_N^3$  over an atomic basin, where  $\mathbf{r}_N$  denotes the distance vector to the nucleus for which a contribution to the shielding tensor is calculated and  $\mathbf{J}^{(1)}(\mathbf{r})$  is the first-order induced current). Here we concentrate on the shielding or deshielding effect of a ring atom on the adjacent proton (see Scheme 6). In **7** and **7-H<sup>+</sup>** a field applied perpendicular to the molecular plane induces currents in the basins of the nitrogen atoms that give rise to a *deshielding* of the adjacent protons (by  $-1.98$  and  $-2.77$  ppm, respectively), a typical diamagnetic ring current effect. For comparison, the corresponding contribution from the carbon basins to the shielding tensors to the protons in benzene amount to  $-3.59$  ppm.<sup>44</sup> On the other hand, in the C–C saturated carbene **9**, the proton attached to the nitrogen atom is actually *shielded* (by 2.13 ppm). Similar effects are found for the protons attached to the carbon atoms of the five-membered ring (Scheme 6). Thus, there is evidence for ring currents in the imidazolium cation **7-H<sup>+</sup>** and, to a smaller extent, also in imidazol-2-ylidene **7**. Clearly, cyclic electron delocalization in these species is less developed than in benzene. However, there is a distinct difference between **7** and **9**. In **9** ring currents as indicators for cyclic electron delocalization can be excluded.

In order to broaden the picture, the anisotropies of the magnetic susceptibility have been calculated for a larger set of model systems using the IGLO method<sup>33</sup> (see Table 4). The

qualitative trends in the magnetic susceptibilities and their anisotropies for **7**, **7-H<sup>+</sup>**, and **9** calculated with IGLO are very similar to the IGAIM results discussed above, and the absolute values agree with a ca. 10% maximum deviation between the two methods. The small  $\Delta\chi$  value calculated for the planar  $C_{2v}$  structure of 1,2-diaminoethane (**17a**) ( $-0.34$  au) shows that the high  $\Delta\chi$  of imidazol-2-ylidene and the imidazolium cation are not due to localized resonance within the NH–CH=CH–NH fragment of the five-membered ring. Saturation of the carbene center in **7** with two hydrogen atoms (**8**) also reduces  $\Delta\chi$  significantly to  $-1.79$  au. Moreover, even an “isolated” HN–C–NH moiety does not cause a large anisotropy, as evident for diaminocarbene **5a** ( $\Delta\chi = -1.64$  au). Finally, the trends in  $\Delta\chi$  for the isostructural silylenes and carbenes are very similar. There is qualitative evidence for ring currents in the C=C unsaturated cyclosilylene **13** ( $\Delta\chi = -6.46$  au) and the corresponding silicenium cation **13-H<sup>+</sup>** ( $\Delta\chi = -5.64$  au) but not for the C–C-saturated cyclosilylene **15** ( $\Delta\chi = -1.41$  au), nor for diaminosilylene **11a** or **14**. However, it is hard to judge from these data whether the absolute degree of cyclic electron delocalization as reflected in the ring currents is more important in the carbene or in the silylene series.

At this point, it is helpful to briefly summarize the state of the discussion: The calculated thermodynamic, structural, and magnetic properties of imidazol-2-ylidene **7** may be interpreted consistently as a reflection of some cyclic electron delocalization, which is less pronounced in the corresponding silylene **13**. Since the theoretical investigation is essentially a comparison between different model systems it is not possible to derive an absolute measure for aromaticity from the presented results. However, from the magnetic properties it is obvious that cyclic electron delocalization is less extensive compared to the aromatic prototype benzene. To cross-check this conclusion, we will now proceed with a detailed analysis of the properties of the charge densities in a series of model system, which are displayed in Scheme 7.

**IV. Properties of the Charge Densities.** For analyzing the bonding between a carbene center and an adjacent amino group, it is useful to briefly summarize the important properties of C–N single and double bonds in simple electronically saturated systems such as methylamine (**17**) and formimine (**18**). As expected, the C–N bond in **18** has a higher covalent bond order ( $\rho(\mathbf{r}_b) = 0.402$ ) as compared to **17** ( $\rho(\mathbf{r}_b) = 0.274$ ).<sup>46</sup> However, the Laplacian at the C–N bond critical point of formimine ( $\nabla^2\rho(\mathbf{r}_b) = -0.61$ ) is *less* negative as compared to methylamine ( $\nabla^2\rho(\mathbf{r}_b) = -0.85$ ), contrary to the trends for the C–C bonds in ethane ( $\nabla^2\rho(\mathbf{r}_b) = -0.671$ ) and ethylene ( $\nabla^2\rho(\mathbf{r}_b) = -1.191$ , both HF/6-311G(d,p)//HF/6-31G(d)). Along with the trends in the atomic charge and the dipole moment on the nitrogen atom (see Table 5), this shows that the  $\pi$ -component brings about higher charge-transfer contributions in the C–N bond compared to a C–C bond. The ellipticity of the C–N bond in formimine is 0.23 with the major axis perpendicular to the plane containing the nuclei, as typical for a  $\pi$ -bonded system. For comparison, the C–C bond ellipticity in ethylene amounts to 0.41. Thus, the prototypical C=N double bond is characterized by (i) substantial ionic contributions and (ii) a lower degree of covalent  $\pi$ -bonding as compared to a typical C=C double bond.

Now consider aminocarbene. The planar minimum structure **19a** is 54.5 kcal/mol (CCSD(T)/6-311G(d,p)//HF/6-31G(d)) more stable than the transition state (TS) for rotation of the

(44) Bader, R. F. W. Personal communication.

(45) (a) Keith, T. A. Ph.D. Thesis, McMaster University, 1993. (b) Keith, T. A.; Bader, R. F. W., manuscript in preparation.

(46) According to ref 35, the covalent bond order  $n$  can be related to the charge density at the bond critical point  $\rho(\mathbf{r}_b)$  via the two-parameter fit  $\ln n = \{A(\rho(\mathbf{r}_b) - B)\}$ . Using HF/6-311G(d,p)//HF/6-31G(d) wave functions for methylamine, formimine, and hydrogen cyanide, a least squares fit to bond orders of 1, 2, and 3 yields  $A = 4.890$  and  $B = 0.270$  for C–N bonds.

**Table 3.** Atomic Contributions to the Magnetic Susceptibility  $\chi$  and Its Anisotropy  $\Delta\chi = \chi_{||} - \chi_{\perp} = \chi_{||} - 0.5(\chi_{\perp 1} + \chi_{\perp 2})$  Calculated by the IGAIM Method (in Atomic Units, Sign Reversed)<sup>a</sup>

molecule	$\Omega$	$\chi_{  }(\Omega)$	$\chi_{\perp}(\Omega)$	$\chi_{  }(\Omega)$	$\chi_{\perp}(\Omega)$	$\Delta\chi_b(\Omega)$	$\Delta\chi_f(\Omega)$	$\chi(\Omega)$
<b>7</b>	C <sup>1</sup>	0.950	-0.107	1.078	0.143	1.057	0.935	0.700
	C <sup>2</sup>	0.624	0.496	1.720	0.362	0.128	1.358	1.354
	N	1.361	1.499	1.657	0.313	-0.138	1.344	2.213
	H <sup>N</sup>	0.142	0.124	0.055	0.038	0.018	0.017	0.174
	H <sup>C</sup>	0.273	0.232	0.192	0.036	0.041	0.156	0.333
sum		5.750	4.595	8.326	1.641	1.155	6.685	8.848
							$\Delta\chi = \chi_{  } - \chi_{\perp} = 7.840$	
<b>7-H<sup>+</sup></b>	C <sup>1</sup>	0.392	0.106	1.421	0.306	0.286	1.115	0.897
	C <sup>2</sup>	0.616	0.464	1.608	0.390	0.152	1.218	1.310
	N	1.521	1.429	1.787	0.346	0.092	1.441	2.286
	H <sup>N</sup>	0.120	0.096	0.059	0.028	0.024	0.031	0.142
	H <sup>C1</sup>	0.203	0.182	0.121	0.038	0.021	0.083	0.254
	H <sup>C2</sup>	0.226	0.199	0.124	0.041	0.027	0.083	0.276
sum		5.561	4.664	8.698	1.954	0.897	6.774	9.161
							$\Delta\chi = \chi_{  } - \chi_{\perp} = 7.641$	
<b>9</b>	C <sup>1</sup>	0.868	-0.403	0.758	0.090	1.271	0.668	0.213
	C <sup>2</sup>	0.514	0.559	1.062	0.630	-0.045	0.432	1.317
	N	1.156	1.655	0.959	0.262	-0.499	0.697	1.983
	H <sup>N</sup>	0.145	0.138	0.059	0.036	0.007	0.023	0.182
	H <sup>C</sup>	0.268	0.258	0.106	0.127	0.010	-0.021	0.351
	H <sup>C</sup>	0.289	0.258	0.119	0.101	0.031	0.018	0.375
sum		5.612	5.333	5.368	2.402	2.966	2.966	8.629
							$\Delta\chi = \chi_{  } - \chi_{\perp} = 3.245$	

<sup>a</sup> Subscripts "b" and "f" indicate basin and surface contributions,<sup>40</sup> respectively. "||" denotes terms induced by a magnetic field perpendicular to the molecular plane, and "⊥", the average contribution from the magnetic field applied along the two axes in the molecular plane.

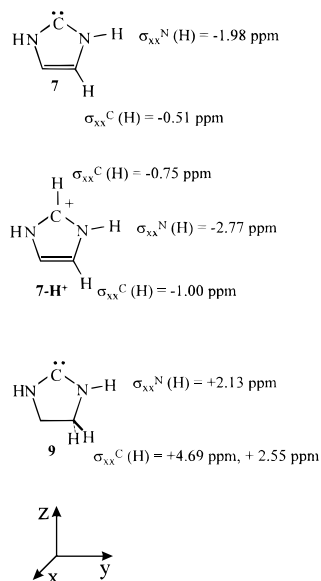
**Table 4.** Magnetic Susceptibilities  $\chi$  and Their Anisotropies  $\Delta\chi = \chi_{||} - \chi_{\perp} = \chi_{||} - 0.5(\chi_{\perp 1} + \chi_{\perp 2})$  Calculated with the IGLO Method (in Atomic Units, Sign Reversed)<sup>a</sup>

molecule	$\chi$	$\chi^{  }$	$\chi^{\perp}$	$\Delta\chi$
<b>5a</b>	6.400	7.495	5.852	1.643
<b>7</b>	10.084	15.537	7.368	8.169
<b>7-H<sup>+</sup></b>	10.337	15.747	7.642	8.105
<b>8</b>	10.526	11.726	9.937	1.789
<b>9</b>	9.874	11.853	8.884	2.969
<b>17a(C<sub>2v</sub>)</b>	9.600	9.832	9.495	0.337
<b>11a</b>	8.716	9.074	8.547	0.526
<b>13</b>	12.337	16.653	10.189	6.463
<b>13-H<sup>+</sup></b>	11.811	15.579	9.937	5.642
<b>14</b>	11.474	12.779	10.821	1.958
<b>15</b>	12.211	13.158	11.747	1.411

<sup>a</sup>  $\chi_{||}$  denotes the contribution to the susceptibility due to a magnetic field perpendicular to the molecular plane and  $\chi_{\perp}$  the average contribution from magnetic fields applied along the two axes in the molecular plane.

C,N bond **19b**, in which the amino group is oriented perpendicularly to the H-C-N moiety. According to resonance arguments, this high rotational barrier can be attributed to *stabilization of the carbene center in 19a* via  $\pi$ -electron donation from the nonbonding "lone pair" on the nitrogen atom into the "empty" p-orbital on the carbenic carbon<sup>6,15,19</sup> ( $H_2H-C-H \leftrightarrow H_2N^+=C^--H$ ), and this expectation is corroborated by atomic-orbital-based analysis methods such as the Mulliken and natural bond orbital (NBO) schemes.<sup>47</sup> However, as noted earlier by MacDougall and Bader,<sup>32</sup> such covalent  $\pi$ -back-donation is *not* reflected in the properties of the charge density of **19a**. In contrast to interactions with genuine  $\pi$ -contributions, in **19a** the major axis of the C-N bond is located *in the plane* of the nuclei and the associated bond ellipticity as well as the charge density at the bond critical point change by less than 10% upon rotation

(47)  $p_z$  population at the carbene center from HF/6-311G(2d,2p) wave functions: **19a**, 0.34 (Mulliken), 0.33 (NBO); **19b**, 0.06 (Mulliken), 0.06 (NBO). Atomic charges: **19a**,  $q(C) = -0.14$  (Mulliken),  $q(N) = -0.13$  (Mulliken),  $q(C) = 0.00$  (NBO),  $q(N) = -0.77$  (NBO); **19b**,  $q(C) = 0.08$  (Mulliken),  $q(N) = -0.36$  (Mulliken),  $q(C) = 0.25$  (NBO),  $q(N) = -0.96$  (NBO).

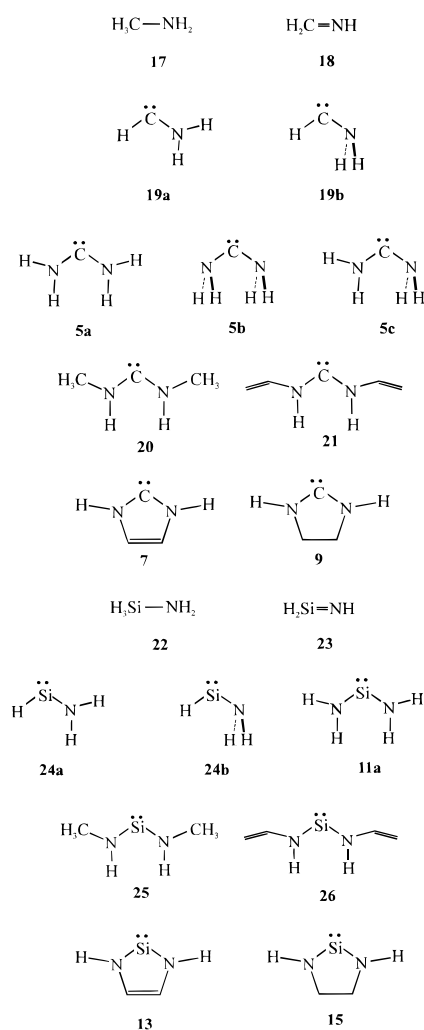
**Scheme 6**

to **19b**. Analysis of the Laplacians at the respective bond critical points (**19a**,  $\nabla^2\rho(r_b) = -0.18$ ; **19b**,  $\nabla^2\rho(r_b) = -1.05$ ) indicates that the C-N interaction is considerably more ionic in the planar conformation, and this interpretation is supported by the reduced charges from the topological analysis and the smaller dipole moment of the nitrogen atom in **19b** compared to **19a** (Table 5). Upon rotation of the C-N bond from **19a** to **19b**, the bond critical point shifts towards the nitrogen atom,<sup>48</sup> thus enlarging the basin of the carbon atom at the cost of the basin of the more electronegative nitrogen atom. Thus, within the framework of the Bader analysis, the rotational barrier in aminocarbenes is due to a *destabilization of the nitrogen atom in 19b* which is not compensated by the concomitant stabilization of the carbene center.<sup>49</sup>

Plots of the Laplacian distributions in these molecules support this picture. Thus, the Laplacian distributions perpendicular to the symmetry planes of the molecules and containing the carbon



Scheme 7



and nitrogen centers for **19a** and **19b** (Figure 3, entries a and b) illustrate graphically that in the “ $\pi$ -plane” the carbon–nitrogen interaction is only weakly perturbed by rotation around the C–N bond. In contrast, the Laplacian distribution for **19a** and **19b** in the symmetry plane of the molecule (Figure 4, entries a and b) clearly demonstrate that the character of the C–N  $\sigma$ -interaction changes from the more ionic to the more covalent regime in going from **19a** to **19b**. Note that the carbenic carbon becomes *less positive* and the nitrogen atom *less negative* upon rotation of the C–N bond from **19a** to **19b**, counterintuitive to the resonance picture ( $\text{H}_2\text{N}-\text{C}-\text{H} \leftrightarrow \text{H}_2\text{N}^+=\text{C}^--\text{H}$ ). A similar behavior has been noted before for the rotational barriers in simple amides<sup>50</sup> and in guanidine<sup>51</sup> and the relation between resonance structures in the classical sense and rotational barriers in these and related compounds is an issue of controversial

(48) The distance between the bond critical point and the carbenic carbon is 0.433 Å in **19a** and 0.590 Å in **19b**.

(49) This interpretation is based on a decomposition of the different energy contributions to the rotational barrier within the atoms-in-molecules picture as described in the following: Bader, R. F. W.; Cheeseman, J. R.; Laidig, K. E.; Wiberg, K. B.; Breneman, C. *J. Am. Chem. Soc.* **1990**, *112*, 6530. Briefly, in **19b** relative to **19a**, the carbon atom is stabilized by 0.2001 au while the destabilization of nitrogen amounts to 0.2970 au. As typical for a rotational barrier, the decrease in the electron–electron and nuclear repulsion is overcompensated by the decrease in the attractive electron–nuclei potential energy  $V_{ne}$ . While for the carbon atom the stabilizing  $V_{ne}$  terms come largely from contributions within its own atomic basin, the corresponding destabilization of the nitrogen atom is dominated by the reduced interatomic  $V_{ne}$  contributions. Further details are available from the authors. email: heineman@zrzsp5.chem.tu-berlin.de.

(50) Wiberg, K. B.; Laidig, K. E. *J. Am. Chem. Soc.* **1987**, *109*, 5935.

(51) Gobbi, A.; Frenking, G. *J. Am. Chem. Soc.* **1993**, *115*, 2362.

discussion.<sup>22,52</sup> In the present case, the relevant question is as to whether  $p_\pi$ – $p_\pi$  resonance actually constitutes the reason for the quite different charge distributions in **19a** and **19b** and thus for the high rotational barrier in aminocarbene. We would like to point out that according to the topological analyses as discussed above this seems not to be the case. Rather, within this interpretation scheme the main electronic differences between **19a** and **19b** concern changes in the *electrostatic* interactions involving the nitrogen atom and the carbene center.<sup>49</sup> This interpretation is fully consistent with the large rotational barrier and the associated bond lengthening (+0.130 Å) in aminocarbene, without reference to resonance arguments. Following MacDougall and Bader,<sup>32</sup> the topological analysis is complementary to the orbital-based delocalization model in that “the magnitude of the atomic back-polarization of [nitrogen] parallels the anticipated consequences of the  $\pi$ -back-donation model”. Despite the particular fascination of this methodological discussion, we will not pursue it further here.

We now address the major question, namely whether linear  $\pi$ -conjugation along the N–C–N framework of planar diaminocarbene **5a** is reflected in Bader’s theory. Such conjugation has been deduced from the calculated differences between the first and second C–N bond rotation barrier<sup>6</sup> (24.8 and 46.4 kcal/mol, at CCSD(T)/6-311G(d,p)//HF/6-31G(d), respectively) in this molecule. Comparison of **5a** with **19a** indicates that the presence of the second amino substituent in **5a** increases the covalent character of the C–N bonds, i.e. the Laplacian at the C–N bond critical point is more negative for **5a** ( $\nabla^2\rho(\mathbf{r}_b) = -0.49$ ; **19a**,  $\nabla^2\rho(\mathbf{r}_b) = -0.18$ ), which also exhibits a smaller dipole moment on nitrogen ( $\mu(\text{N}) = 0.393$ ; **19a**,  $\mu(\text{N}) = 0.494$ ). Consistently, each of the nitrogen atoms in **19a** shows two nonbonded maxima in the VSCC (one above and one below the plane of the nuclei). The magnitude of the C–N bond ellipticity in **5a** ( $\epsilon = 0.33$ ) is slightly reduced compared to **19a** ( $\epsilon = 0.45$ ),<sup>53</sup> but the major axis of the C–N bond in diaminocarbene is still *in the molecular plane*. Also the properties of the charge densities in the rotated conformers of diaminocarbene **5b** (a second-order saddle point) and **5c** (a rotational TS) are quite similar to the respective data for the planar and the perpendicular conformation of aminocarbene, **19a** and **19b**. Thus, the basic properties of the C–N bonds in diaminocarbene **5a** resemble those of aminocarbene **19a**, and according to the theory of “atoms-in-molecules” there is no clearcut indication for an allyl-type delocalization of  $4\pi$ -electrons along the N–C–N framework of **5a**.

A quite different electronic situation is encountered in the corresponding C-protonated carbenes **19-H<sup>+</sup>** and **5-H<sup>+</sup>**. In particular, their C–N bond ellipticities merit attention: In contrast to **19a**, **19a-H<sup>+</sup>** does not exhibit preferential charge accumulation in the molecular plane with respect to the out-of-plane direction ( $\epsilon = 0.00$ ) and in **5a-H<sup>+</sup>** the principal axis is even *perpendicular* to the molecular plane, thus clearly showing the effect of  $\pi$ -electron release from the nitrogen substituent to the carbenium center. This conclusion is corroborated by inspection of the Laplacian distribution for **19a-H<sup>+</sup>** in the  $\pi$ -plane (Figure 3c), which exhibits an increased aggregation of the electron density in the region between carbon and nitrogen compared to **19a** (Figure 3a). The more negative values of the Laplacians of the total charge density at the bond critical points as well as the smaller dipole moments of the nitrogen atoms indicate that the C–N interactions in the protonated carbenes

(52) Wiberg, K. B.; Cheeseman, J. R.; Ochterski, J. W.; Frisch, M. J. *J. Am. Chem. Soc.* **1995**, *117*, 6535 and references cited therein.

(53) **19a** has a larger negative curvature perpendicular to the molecular plane ( $\lambda_1 = -0.892$ ) and a smaller negative curvature along the major axis ( $\lambda_2 = -0.614$ ) compared to **5a** ( $\lambda_1 = -0.835$ ,  $\lambda_2 = -0.630$ ).

**Table 5.** Analysis of Atomic and Bond Properties in the C–N Bonded Model Systems Shown in Scheme 7<sup>a</sup>

	$R_e$ (C–N)	$\rho(\mathbf{r}_b)$ (C–N)	$\nabla^2\rho(\mathbf{r}_b)$ (C–N)	$\epsilon$ (C–N) <sup>b</sup>	$q(\text{C})$	$q(\text{N})$	$\mu(\text{N})$	VSCC(N)	$Q_{zz}(\text{C})$
<b>5a</b>	1.337	0.322	−0.49	0.33	1.18	−1.37	0.393	5	−3.14 <sup>d</sup>
<b>5b</b>	1.441	0.293	−1.08	0.41	0.94	−1.18	0.159	4	
<b>5c</b>	1.313/1.452	0.334/0.242	−0.36/−0.99	0.28/0.37	1.05	−1.39/−1.16	0.490/0.150	4/3	
<b>5a-H<sup>+</sup></b>	1.299	0.367	−0.88	0.05 $\perp$	1.62	−1.39	0.353	3	
<b>5b-H<sup>+</sup></b>	1.370	0.351	−1.35	0.16	1.22	−1.18	0.032	4	
<b>5c-H<sup>+</sup></b>	1.273/1.379	0.378/0.337	−0.52/−1.26	0.05 $\perp$ /0.14	1.43	−1.39/−1.19	0.481/0.066	3/4	
<b>7</b>	1.352	0.312	−0.37	0.22	1.06	−1.50	0.268	3	−2.42
<b>7-H<sup>+</sup></b>	1.313	0.370	−1.23	0.03 $\perp$	1.42	−1.49	0.238	3	
<b>9</b>	1.343	0.323	−0.55	0.30	1.14	−1.45	0.351	4	−2.84
<b>9-H<sup>+</sup></b>	1.298	0.370	−0.88	0.07 $\perp$	1.57	−1.48	0.325	3	
<b>17</b>	1.453	0.274	−0.85	0.02 <sup>c</sup>	0.60	−1.12	0.186	4	
<b>18</b>	1.251	0.402	−0.61	0.23 $\perp$	0.97	−1.30	0.478	3	
<b>19a</b>	1.309	0.330	−0.18	0.45	0.63	−1.35	0.494	3	
<b>19b</b>	1.439	0.292	−1.05	0.49	0.51	−1.15	0.166	4	
<b>19a-H<sup>+</sup></b>	1.263	0.381	−0.41	0.00	0.94	−1.37	0.481	3	
<b>19b-H<sup>+</sup></b>	1.356	0.358	−1.38	0.18	0.74	−1.15	0.049	4	
<b>20</b>	1.335	0.323	−0.46	0.31	1.17	−1.47	0.393	5	−3.10
<b>21</b>	1.339	0.322	−0.46	0.33	1.17	−1.52	0.358	3	−3.12

<sup>a</sup>  $R_e$  denotes the C–N bond distance (HF/6-31G(d)),  $\rho(\mathbf{r}_b)$  the charge density at the C–N bond critical point,  $\nabla^2\rho(\mathbf{r}_b)$  the Laplacian at this bond critical point,  $\epsilon$  the bond ellipticity,  $q(\Omega)$  the atomic charges ( $\Omega = \text{C}, \text{N}$ ),  $\mu(\text{N})$  the atomic dipole moment of nitrogen, VSCC(N) the number of maxima in the valence-shell charge concentration of the nitrogen atom, and  $Q_{zz}$  the  $zz$ -component of the atomic quadrupole moment at the carbene center ( $z$ -axis = axis of rotation). All values are given in atomic units, except for the  $R_e$  values which are given in angstroms. <sup>b</sup> The major axis of the bond lies in the molecular plane, except for those values signed with “ $\perp$ ”, where the major axis of the bond is perpendicular to molecular plane. <sup>c</sup> Major axis in the symmetry plane of the pseudo-staggered  $C_s$  minimum conformation. <sup>d</sup> At optimum geometry with  $\theta(\text{N–C–N}) = 104.1^\circ$ ,  $Q_{zz}(\text{C}) = -2.72$ ; at optimum geometry with  $\theta(\text{N–C–N}) = 101.0^\circ$ ,  $Q_{zz}(\text{C}) = -2.55$ .

(i.e. the respective carbenium ions) have less ionic and more covalent contributions as compared to the neutral species, thereby substantiating the view that in the carbenium ions significant  $\pi$ -electron delocalization is operative. Consequently, the charges in bond ellipticities upon rotation of the C–N bonds are also more pronounced as compared to the neutral carbene cases. Again, it is helpful to examine the graphical representation of the relevant Laplacian distributions shown in Figure 3. First, note that in the  $\pi$ -plane  $\nabla^2\rho(\mathbf{r})$  for the perpendicular rotational transition states **19b** and **19b-H<sup>+</sup>** appear to be very similar. Thus, there is indeed a significant change in N→C  $\pi$ -back-donation upon internal rotation of **19-H<sup>+</sup>** (Figure 3c,d), which is not apparent for the neutral aminocarbene (Figure 3a,b). In contrast, the Laplacian distributions in the molecular symmetry plane are qualitatively similar for the two relevant stationary points of the aminomethyl cation (Figure 4c,d) and aminocarbene (Figure 4a,b). This leads to the conclusion that from the properties of the charge density, the origins for the rotational barriers of aminocarbene and its carbenium ion analog differ by an additional contribution from  $p_\pi$ – $p_\pi$  resonance in the latter species. However, this difference is not strongly reflected in the activation energies for internal rotations in protonated mono- and diaminocarbene (**19a-H<sup>+</sup>**, 74.7 kcal/mol; **5a-H<sup>+</sup>**, first C–N bond rotation 28.9 kcal/mol, second C–N bond rotation 86.7 kcal/mol, CCSD(T)/6-311G(d,p)//HF/6-31G(d)), which are not substantially higher compared to the corresponding neutral carbenes (see above). *Cum grano salis*, this comparison allows to bracket the stabilization of protonated aminocarbenes by  $p_\pi$ – $p_\pi$  resonance is 10–20 kcal/mol.

Substitution of one hydrogen atom in the amino groups by an alkyl or a vinyl group has only a minor effect on the characteristics of the charge density (i.e. compare bis(methylamino)carbene (**20**) and bis(vinylamino)carbene (**21**) with **5a**). Apart from the properties related to the question of electron delocalization involving the carbene center, some  $\pi$ -type interactions between the vinyl group and the nitrogen atom can be deduced from the missing nonbonded maxima of the VSCC at the nitrogen atom in **21**. Similar to diaminocarbene, these are found in bis(methylamino)carbene (**20**), indicating that any allyl-type  $\pi$ -interaction between the carbene center and the two nitrogen atoms is weaker as compared to conjugation between

the nitrogen and the vinyl group in **21**. This conclusion is supported by comparing  $Q_{zz}(\text{C})$  values, the  $zz$ -component of the atomic quadrupole tensor<sup>54</sup> at the carbene center, for a series of model systems. This quantity describes the toroidal shape of the charge density and, in the special case of the carbenes, provides a measure for the population of the “empty”  $\pi$ -orbital relative to the in-plane  $n_\sigma$ -orbital.<sup>55</sup> The calculated negative  $Q_{zz}$  values (Table 5) indicate that charge density around the divalent carbon atom is preferentially accumulated in the molecular plane, as expected for singlet carbenes. Furthermore,  $Q_{zz}$  has nearly the same value for **5a**, **20**, and **21**, which supports the conclusion that *N*-alkyl and -vinyl substituents do not affect delocalization and resonance along the N–C–N linkage in diaminocarbenes.

On the basis of these results one can now analyze the charge distributions in imidazol-2-ylidene **7** and imidazolin-2-ylidene **9**, the model systems closest to the Arduengo (**1**) and Wanzlick (**2**) type cyclocarbenes. **9** is to be compared to diaminocarbene **5a** and its *N*-methylated derivative **20**. With regard to the issue of  $\pi$ -electron delocalization, the molecular charge distributions (Table 5). Each nitrogen atom exhibits a nonbonded maximum in the valence shell charge concentration. The slightly smaller  $Q_{zz}$  values for **9** is due to the smaller bond angle  $\theta(\text{N–C–N})$  in the ring ( $104.1^\circ$ , compared to  $112.5^\circ$  and  $113.1^\circ$  in **5a** and **20**, see footnote *c* to Table 5). Similar to the noncyclic aminocarbenes, protonation of imidazolin-2-ylidene (**9** → **9-H<sup>+</sup>**) enhances the  $p_\pi$ – $p_\pi$  interaction along the C–N bonds, as apparent from the higher value of the charge density at the C–N bond critical point of **9-H<sup>+</sup>** (see Table 5) and a change in the direction of the major axis of the C–N bond (*in* the N–C–N plane in **9** but *perpendicular* to the N–C–N moiety in **9-H<sup>+</sup>**).

Finally, we consider the C=C unsaturated imidazol-2-ylidene carbene **7**. To analyze the importance of conjugation, this molecule should now be compared to its C–C saturated counterpart **9**. The overall differences in the properties of the

(54) The orientation is chosen such that the molecule lies in the  $yz$  plane with the  $z$ -axis being the 2-fold axis of rotation.

(55) For applications of this concept to substituted benzenes, see: (a) Bader, R. F. W.; Chang, C. *J. Phys. Chem.* **1989**, *93*, 2946. (b) Bader, R. F. W.; Chang, C. *J. Phys. Chem.* **1989**, *93*, 5095. (c) Reference 21, p 205ff.

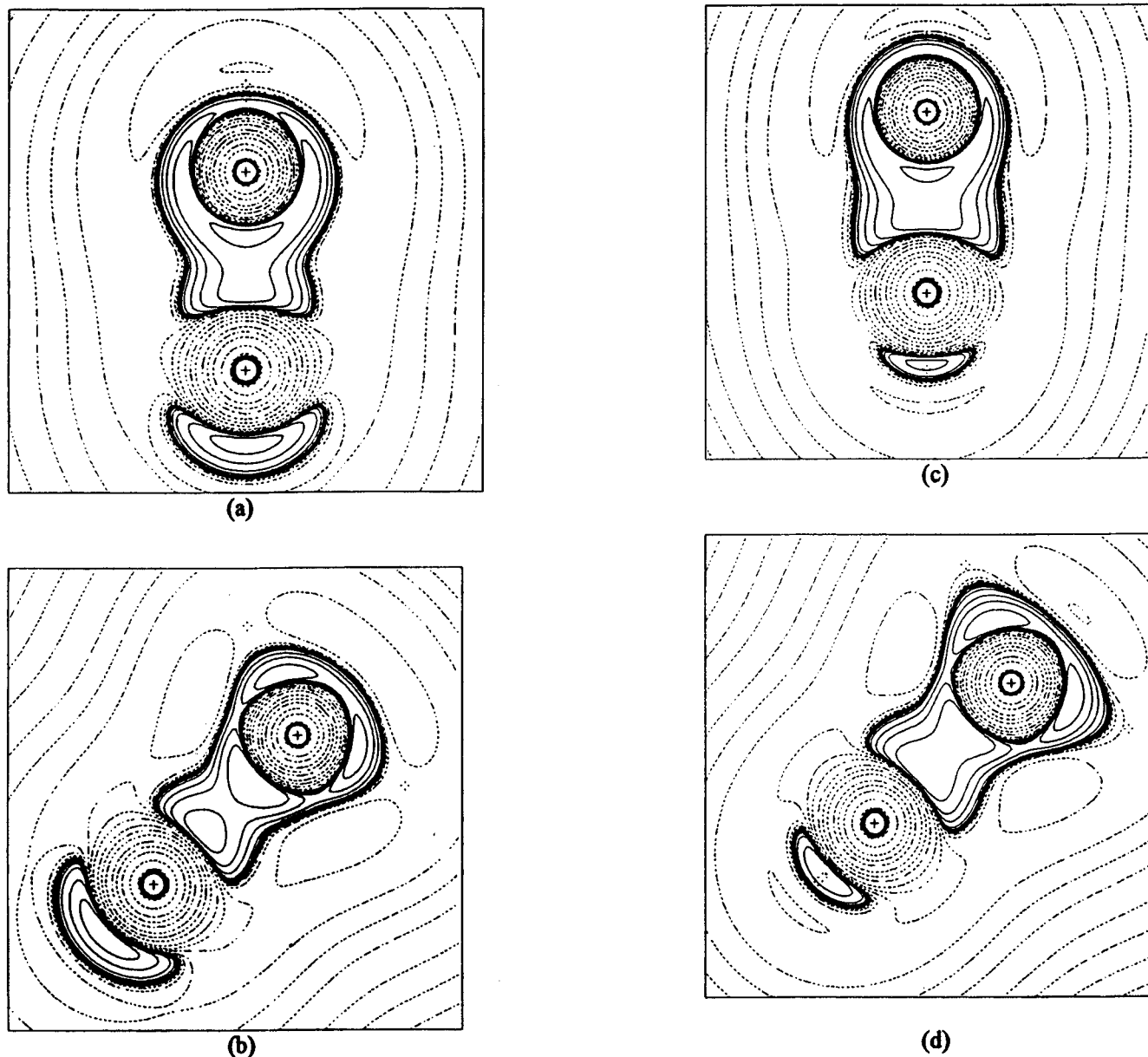


**Figure 3.** Contour plots of the Laplacian distributions  $\nabla^2\rho(\mathbf{r})$  in the plane perpendicular to the molecular symmetry plane and containing the C,N bond for (a) **19a**, (b) **19b**, (c) **19a-H<sup>+</sup>**, and (d) **19a-H<sup>+</sup>**. Solid and dotted lines designate regions of local charge concentration and depletion, respectively.

charge density between these two model systems for the stable carbenes **1** and **2** are small. However, there is a certain trend to be recognized: Electrostatic interactions via localized charge distributions are less important in **7** compared to **9**, as reflected in the topological charges of the carbon and nitrogen atoms and the atomic dipole moment of the nitrogen centers (Table 5). In both species, the major axis of the C–N bond is in the plane of the nuclei, contrary to the C–X bond in the “aromatic” five-membered heterocycles furan (X = O) and thiophene (X = S).<sup>36</sup> However, the slightly reduced C–N bond ellipticity in **7** ( $\epsilon = 0.22$ , compared to  $\epsilon = 0.30$  in **9**) reflects a higher importance of out-of-plane charge density in the C–N interaction.<sup>56</sup> Furthermore,  $Q_{zz}(\text{C})$  is less negative in **7** ( $Q_{zz} = -2.42$ ) as compared to **9** ( $Q_{zz} = -2.84$ ) and the geometry differences (i.e. the larger N–C–N angle in **9** ( $104.1^\circ$ ) compared **7** ( $101.0^\circ$ )) cannot quantitatively account for this trend (Table 5, footnote c). The relevant Laplacian distributions plotted in Figure 5 show for **7** a more spherical lone-pair shape and a spatially more compact region of electron density depletion at the carbenic carbon above and below the molecular plane as compared to **9**.

All these data suggest that there is a *small but detectable* degree of  $\pi$ -electron delocalization along the N–C–N moiety in imidazol-2-ylidene **7** as compared to the C–C saturated analog **9**.

If the increased electron delocalization along the C–N bond in **7** is really cyclic in origin, this should also be apparent in the properties of the charge density along its N–C'–N “backbone”. To test this point, we compare **7** to 1,2-diaminoethane **17a** in the planar  $C_{2v}$  conformation (see Scheme 8).

First, note that each nitrogen atom in **17a** shows a symmetric pair of nonbonded maxima in their VSCCs, reminiscent of nonbonding “lone pairs”, a feature which is absent in **7**. Furthermore, the ellipticity of the C'–C' bond increases and that of the C'–N bond decreases from **7** to **17a**. In both cases, the major axes are perpendicular to the molecular plane, as expected for bonds with  $\pi$ -character. The observed decrease

(56) The decrease of  $\epsilon$  is due to a smaller curvature  $\lambda_1$  along the minor axes perpendicular to the molecular plane (**7**,  $\lambda_1 = -0.747$ ; **9**,  $\lambda_1 = -0.827$ ) while the curvatures  $\lambda_2$  along the major axis are almost identical (**7**,  $\lambda_2 = -0.611$ ; **9**,  $\lambda_2 = -0.634$ ).

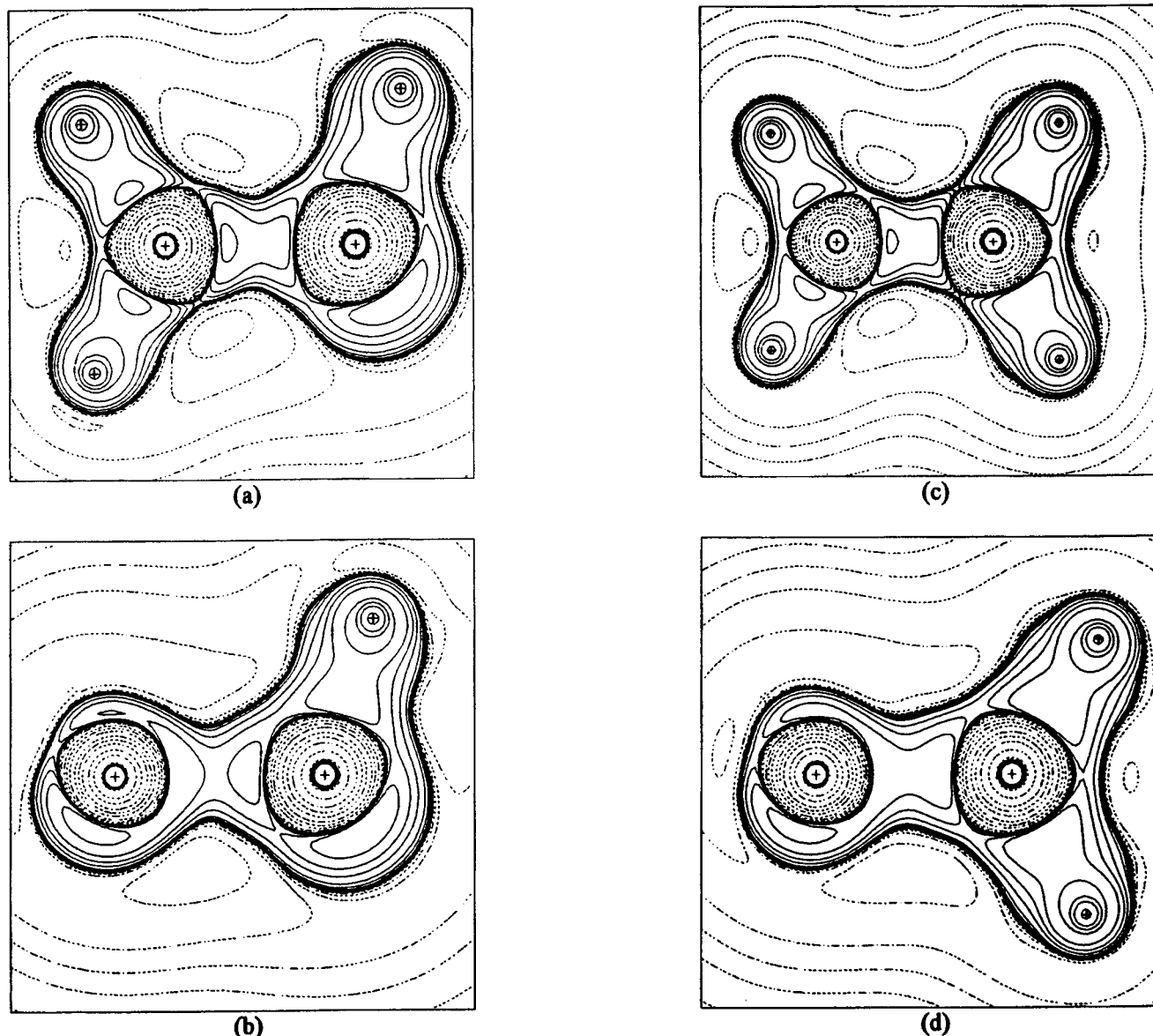


**Figure 4.** Contour plots of the Laplacian distributions  $\nabla^2\rho(\mathbf{r})$  in the molecular symmetry plane for (a) **19a**, (b) **19b**, (c) **19a-H<sup>+</sup>**, and (d) **19a-H<sup>+</sup>**.

in the  $\pi$ -character of the formal C=C double bond and the increase of the  $\pi$ -contributions to the formal C–N single bonds are fully consistent with cyclic  $\pi$ -electron resonance in imidazol-2-ylidene **7**. Thus, the analyses of both the N–C–N moiety and the N–C′=C′–N backbone *consistently indicate some degree of cyclic electron delocalization* in **7**. However, we would like to stress that compared to the large effects discussed above for the thermodynamic and magnetic properties (sections I and III), the *reflection of the additional delocalization in 7 within the “atoms-in-molecules” picture is small*. This becomes even more evident when the imidazolium cation **7-H<sup>+</sup>**<sup>10,11,57</sup> is analyzed. This molecule has undoubtedly the most delocalized  $\pi$ -electron system among all species considered so far, as, for example, evident from the perpendicular direction for the major axis associated with the carbene–nitrogen bond and the high covalent bond order between these two atoms ( $\rho(\mathbf{r}_b) = 0.370$  in **7-H<sup>+</sup>** as compared to  $\rho(\mathbf{r}_b) = 0.312$  in **7**; see also Table 5 for **17** and **18**). Moreover, note that the atomic charge of the carbene center in **7** increases by only +0.36e upon protonation, compared with +0.44e and +0.43e for the protonation of diaminocarbene **5a** and imidazolin-2-ylidene **9**, consistent with

(57) A bis(carbene) proton complex involving two imidazol-2-ylidenes has recently been reported: ref 23r.

a better delocalization of the positive charge in the unsaturated imidazol-2-ylidene ring system. Even more convincing is the graphical representation of the Laplacian distribution in **7-H<sup>+</sup>** (Figure 5c), which exhibits a significantly more pronounced charge accumulation in the  $\pi$ -plane of the C,N bond as compared to the cyclocarbenes **7** and **9**. We conclude that for all systems considered here, the topological analysis indicates enhanced  $p_\pi$ – $p_\pi$  resonance in carbenium cations (i.e. protonated carbenes) as compared to the corresponding neutral carbenes.

We now turn to the amino-substituted silylenes. Let us examine first the simplest Si–N single and double bonds. Aminosilane **22** and methylamine **17** differ significantly in many aspects of their molecular charge densities. Most differences can be attributed to the larger electronegativity difference  $\Delta\eta$  between silicon and nitrogen ( $\Delta\eta(\text{Si/N}) = 1.02$ ) as compared to carbon and nitrogen ( $\Delta\eta(\text{C/N}) = 0.49$ ). For example, this results in an atomic dipole moment nearly 4 times higher in **22** than in **17** and a *positive* value for the Laplacian of  $\rho(\mathbf{r})$  at the Si–N bond critical point, indicating the ionic character of the Si/N interaction. The same criteria indicate a further increase of the Si–N bond ionicity in going from the singly bonded **22** to the formally doubly bonded silaimine **23**. The increase in the Si–N bond ellipticity  $\epsilon$  between **22** and **23** of 0.11 (major

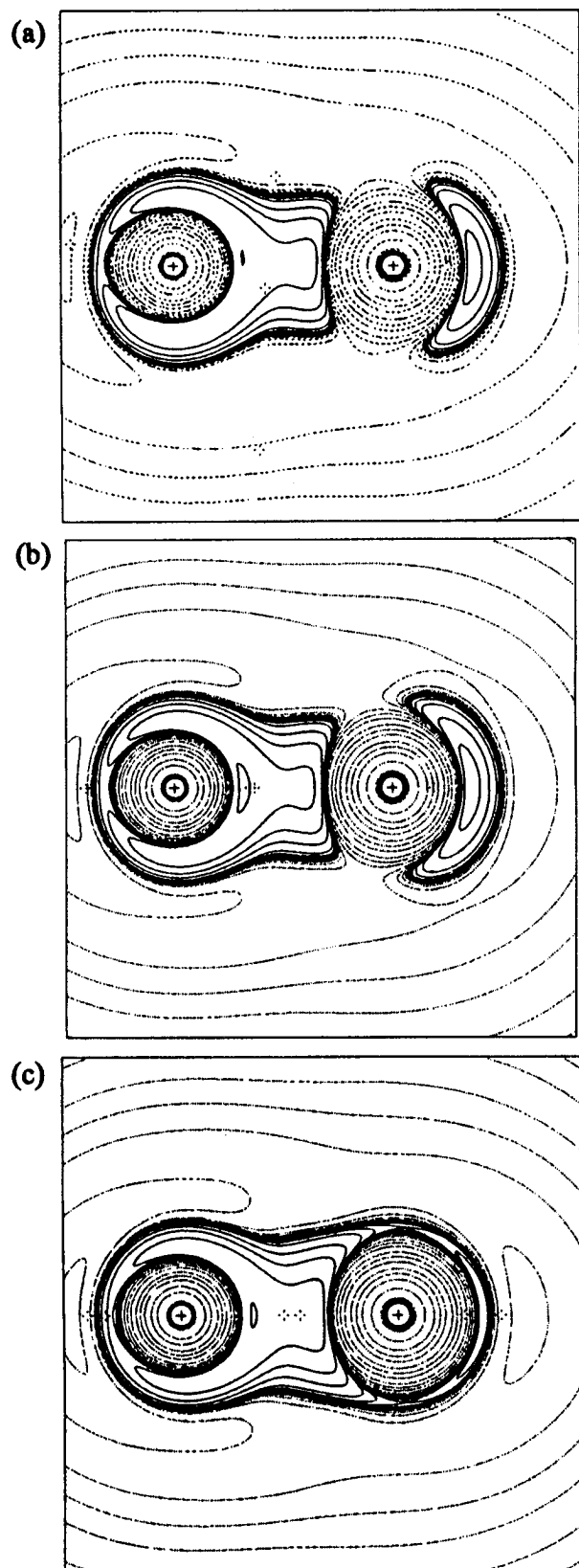


**Figure 5.** Contour plots of the Laplacian distributions  $\nabla^2\rho(\mathbf{r})$  in the plane perpendicular to the molecular symmetry plane and containing the C,N bond for (a) **9**, (b) **7**, and (c) **7-H<sup>+</sup>**.

axis perpendicular to the molecular plane) is smaller than in the carbon analogs (0.21). This is consistent with the common view that covalent  $\pi$ -bonds between silicon and first period elements are intrinsically weaker than those among elements of the first period themselves.<sup>18</sup>

### Scheme 8

C'-C'	$R_e$	1.332	1.329
	$\rho(r_b)$	0.356	0.355
	$\epsilon$	0.49	0.60
C'-N	$R_e$	1.387	1.392
	$\rho(r_b)$	0.306	0.292
	$\epsilon$	0.10	0.07

All Si–N bond properties in the planar minimum conformation of aminosilylene **24a** are reminiscent of the electronic situation in silylamine **22**. One difference between these two molecules is that the nonbonded fourth maximum in the nitrogen VSCC is missing in **24a**, a feature which aminosilylene and aminocarbene have in common and which relates to the strong polarization of the nitrogen atom. Note, that the ionicity of the Si–N bond in **24a** is higher than that of the C–N bond in planar aminocarbene **19a**, as apparent from the Laplacians of the charge density at the bond critical points (see Tables 5 and 6). Upon rotation around the Si–N bond (**24a**  $\rightarrow$  **24b**), the charge of the silicon atom hardly changes, and in general the differences in atomic and bonding properties between the two conformers are significantly smaller than for the carbene analogs **19a** and **19b**. Consistently, the rotation barrier around the Si–N bond in **24** (26.5 kcal/mol, CCSD(T)/6-311G(d,p)//HF/6-31G-(d)) is only ca. half of the corresponding values for **19** (54.5 kcal/mol). According to the topological charge density analysis, the origin of this rotational barrier is *not*  $p_\pi$ - $p_\pi$  overlap and resonance but rather the more advantageous *electrostatic* interactions for the silicon and the nitrogen atoms in the planar conformer **24a**. The properties of the charge density of planar (minimum structure) diaminosilylene **11a** are also quite similar to those of silylamine **22**. Contrary to the isostructural carbenes (see above), the nonbonding maxima in the VSCCs of the nitrogen atoms do not reappear when a second amino group is present (e.g. in **11a**). There are no indications for linear, allyl-type delocalization of  $\pi$ -electrons along the N–Si–N moiety of **11a**. The same applies to bis(methylamino)- and bis(vinylamino)silylene **25** and **26** (see Table 6), indicating only minor substituent effects on the electronic characteristics of the Si–N bonds of diaminosilylenes.

Finally, we arrive at **13** and **15**, the model systems for the isolable C=C-unsaturated (**3**) and C–C-saturated (**4**) cyclosilylenes. The atomic and bond properties along the N–Si–N linkage in the C–C-saturated species **15** are very similar to those in diaminosilylene **11a**. The most significant difference is the lower value of the atomic quadrupole component  $Q_{zz}(\text{Si})$  in **15**. As in the carbene case, this can be attributed to the smaller N–Si–N valence angle in the five-membered ring (**15**, 89.2°; **11a**, 100.4°). The differences in the molecular charge distributions between **15** and **13** are not very pronounced, either. Introduction of the double bond into the five-membered ring shows qualitatively the same effects as for the homologous carbenes: A decrease in the dipole moment of the nitrogen atoms and in the charge of the silicon atom and a reduction of 1.04 in  $Q_{zz}(\text{Si})$  for which one may estimate a contribution of 0.23 from geometry effects. Note, however, that the ellipticity  $\epsilon$  of the Si–N bond is hardly influenced by the presence of the double bond in the five-membered ring. The “backbone” properties of the cyclic silylene **13** (C'=C' bond,  $\epsilon = 0.51$ ,  $\rho(r_b) = 0.357$ ; C'–N bond,  $\epsilon = 0.08$ ,  $\rho(r_b) = 0.297$ ) are

**Table 6.** Analysis of Atomic and Bond Properties in the Si/N-Bonded Model Systems Shown in Scheme 7<sup>a</sup>

	$R(\text{Si}-\text{N})$	$\rho_{\text{b}}(\text{Si}-\text{N})$	$\nabla^2\rho_{\text{b}}(\text{Si}-\text{N})$	$\epsilon(\text{Si}-\text{N})$	$q(\text{Si})$	$q(\text{N})$	$\mu(\text{N})$	VSCC(N)	$Q_{\text{zz}}(\text{Si})$
<b>11a</b>	1.716	0.126	0.74	0.17 $\perp$	1.64	-1.59	0.666	3	-4.66
<b>13</b>	1.743	0.120	0.70	0.17 $\perp$	1.51	-1.69	0.541	3	-2.97
<b>15</b>	1.721	0.126	0.74	0.15 $\perp$	1.61	-1.66	0.660	4	-4.01
<b>22</b>	1.724	0.129	0.70	0.14 <sup>b</sup>	3.07	-1.59	0.625	4	
<b>23</b>	1.573	0.172	1.24	0.25 $\perp$	2.92	-1.83	1.032	3	
<b>24a</b>	1.706	0.128	0.78	0.16 $\perp$	1.57	-1.59	0.692	3	
<b>24b</b>	1.773	0.121	0.56	0.15	1.60	-1.56	0.632	4	
<b>25</b>	1.718	0.126	0.74	0.20 $\perp$	1.63	-1.67	0.670	3	-4.86
<b>26</b>	1.731	0.123	0.71	0.17 $\perp$	1.64	-1.71	0.600	3	-4.38

<sup>a</sup> See Table 5 for the employed abbreviations. <sup>b</sup> The major axis lies the symmetry plane of the pseudo-staggered  $C_3$  minimum conformation.

numerically almost identical to those in the homologous carbene **7** (see Scheme 8).

In summary, according to the topological charge density analysis the trends in the series of model silylene systems are qualitatively similar, but less pronounced, than for the isostructural carbenes. According to this analysis, cyclic electron delocalization in the C=C-unsaturated cyclosilylene **13** is less developed than in the C=C-unsaturated carbene **7**, where the effect was already small. The smaller conjugation in the silicon series indicated by the topological charge density analysis is consistent with the conclusions based on the thermodynamic, structural and magnetic criteria discussed in sections I–III.

**V. Ionization Processes.** Arduengo and co-workers have compared the photoelectron (PE) spectra of an imidazol-2-ylidene (**1**, R = *tert*-butyl) with its higher silicon and germanium analogs.<sup>9</sup> Accompanying density-functional calculations showed that in the carbene the lowest-energy ionization process involves removal of an electron from the “lone pair” orbital localized at the carbenic carbon. In the corresponding silylene (**3**, R = *tert*-butyl), silicon lone-pair ionization corresponds to the second lowest band in the PE spectrum, and ionization from a  $\pi$ -type orbital with contributions from all of the five-membered ring atoms was found to be energetically more favorable. Removal of a lone pair electron from either **1** or **3** gives rise to a  $^2A_1$  state of the corresponding cation–radical **1**<sup>+</sup> or **3**<sup>+</sup>, whereas ionization from the  $\pi$ -orbital generates the cation–radical in the  $^2B_1$  state. In the following discussion, these two ionization processes are analyzed for the hydrogen-substituted model systems **7** and **13**. Substitution of the hydrogen atoms by *tert*-butyl groups is expected to influence the absolute ionization energies but not the ordering of the electronic states of the cation radicals.

Examining the Hartree–Fock orbital energies  $\epsilon_{i,\text{HF}}$  as well as the relative energies of the two cation–radical states (Table 7), it is apparent that in imidazol-2-ylidene **7** lone-pair ionization violates Koopmans’ theorem<sup>58</sup> ( $\text{IE}_i \cong -\epsilon_{i,\text{HF}}$ , where  $\text{IE}_i$  denotes the ionization energy for an electron from an orbital with the orbital energy  $\epsilon_{i,\text{HF}}$ ) in the following sense: The calculated energies of the highest  $a_1$  (lone pair) and  $b_1$  ( $\pi$ -type) orbitals in **7** are -9.5 and -8.7 eV, respectively. The  $b_1$  orbital corresponds to the highest occupied molecular orbital (HOMO); the  $a_1$  is the second highest molecular orbital.<sup>59</sup> Thus, on the basis of Koopmans’ theorem, one would expect that ionization of a lone-pair electron is about 1 eV *less* favorable as compared to removal of an electron from the  $\pi$ -type  $b_1$  orbital. Experimentally,

(58) Koopmans, T. *Physica* **1934**, *1*, 104.

(59) The authors of ref 9 denote the lone-pair  $a_1$  orbital as the HOMO of the C=C-unsaturated carbene on the basis of an application of Koopmans’ theorem for the Kohn–Sham orbitals of density-functional theory. See: (a) Janak, J. F. *Phys. Rev. B* **1978**, *18*, 7165. (b) Slater, J. C. *Adv. Quantum Chem.* **1972**, *6*, 1. Note that there is a difference in the physical meaning of Hartree–Fock and Kohn–Sham orbital energies. For a discussion of this point, see, for example: (c) Jones, R. O.; Gunnarsson, O. *Rev. Mod. Phys.* **1989**, *61*, 689. (d) Parr, R. G.; Yang, W. *Density Functional Theory of Atoms and Molecules*; Oxford University Press: New York, 1989.

**Table 7.** Theoretical and Experimental Ionization Energies (in eV) from the Highest Orbitals of  $a_1$  (Carbene/Silylene Lone Pair Orbital) and  $b_1$  ( $\pi$ -Type Orbital) Symmetry of the C=C-Unsaturated Cyclocarbenes and -silylenes **7** and **13**<sup>a</sup>

ionization from orbital	<b>7</b>		<b>13</b>	
	$a_1$	$b_1$	$a_1$	$b_1$
$-\epsilon_{i,\text{HF}}^c$	9.5	8.7 <sup>d</sup>	9.1	7.7 <sup>d</sup>
$\Delta\text{PUHF}/6-31\text{G(d)}$	6.9	7.6	7.6	6.6
$\Delta\text{PUMP2}/6-31\text{G(d)}$	7.7	8.8	8.3	7.6
$\Delta\text{PUMP3}/6-31\text{G(d)}$	7.7	8.6	8.4	7.4
$\Delta\text{PUMP4}/6-31\text{G(d)}$	7.8	8.7	8.4	7.5
$\Delta\text{CCSD(T)}/6-31\text{G(d)}$	7.8	8.6	8.4	7.4
exp ( <b>1</b> with R = <i>tert</i> -butyl) <sup>9</sup>	7.7	8.2	8.2	7.0

<sup>a</sup>  $\Delta$  values correspond to vertical ionizations and were obtained by subtracting the total energies<sup>b</sup> (using the spin-projection method<sup>31</sup> for UHF and MP $n$ ) computed at the HF/6-31G(d) geometry of the corresponding neutral molecule. <sup>b</sup> Expectation values of  $S^2$ : 0.863 ( $7^+$ ,  $^2A_1$ ); 0.766 ( $7^+$ ,  $^2B_1$ ); 1.011 (**13**<sup>+</sup>,  $^2A_1$ ); 0.756 (**13**<sup>+</sup>,  $^2B_1$ ). <sup>c</sup> Negative Hartree–Fock orbital energies (6-31G(d) basis) of the neutrals. <sup>d</sup> Highest occupied molecular orbital (HOMO) of the neutral in the Hartree–Fock approximation.<sup>59</sup>

tally, one finds that the  $b_1$  ionization in **1** (R = *t*-butyl) occurs at 8.2 eV,<sup>9</sup> in reasonable agreement with the calculated  $b_1$  orbital energy of **7**. In contrast, for the lone-pair ionization there is an unexpected difference of nearly 2 eV between the calculated  $a_1$  orbital energy in **7** of 9.5 eV and the experimental value of 7.7 eV<sup>9</sup> for **1** (R = *tert*-butyl).

Koopmans’ theorem implies that the orbitals of the cation are the same as in the neutral molecule. However, in reality the electron distribution in the cations relaxes upon ionization. On the other hand, the Hartree–Fock approximation, which yields the orbital energies  $\epsilon_{i,\text{HF}}$ , does not include electron correlation, which is expected to stabilize the neutral molecule more than the cation. Thus, Koopmans’ theorem is valid only in cases where these two sources of error fortuitously cancel each other.<sup>60</sup>  $\Delta\text{UHF}$  calculations (i.e. subtracting the independently calculated Hartree–Fock energies of the neutral and the cation) usually give less accurate theoretical ionization energies in these cases and correlation energies have to be explicitly evaluated for both the neutral and its cation to remediate the shortcomings of the Hartree–Fock approach. This situation is met for the  $b_1$  ionization from **7** (Table 7): A  $\Delta\text{UHF}$  calculation yields a lower ionization energy (7.6 eV) than the value based on Koopmans’ theorem (8.7 eV). Explicit inclusion of electron correlation, which seems to be converged within the employed basis at the  $\Delta\text{PUMP4}$  and  $\Delta\text{CCSD(T)}$  levels of theory, gives nearly the same result as Koopmans’ theorem, which can thus be regarded as being valid for the ionization of an electron from the  $b_1$  orbital of **7**.

On the other hand, in the case of  $a_1$  ionization the relaxation of the wave function in the cation is unexpectedly large such that the  $\Delta\text{UHF}$  result (6.9 eV) differs from the corresponding

(60) Szabo, A.; Ostlund, N. S. *Modern Quantum Chemistry*; McGraw-Hill: New York, 1982.

**Table 8.** Properties of the Charge Density<sup>a</sup> for Neutral and Cationic Cyclocarbenes and -silylenes **7** (E = C) and **13** (E = Si)<sup>b</sup>

	<b>7</b>		<b>7<sup>+</sup></b>		<b>13</b>		<b>13<sup>+</sup></b>	
	<sup>1</sup> A <sub>1</sub>	<sup>2</sup> A <sub>1</sub>	<sup>2</sup> B <sub>1</sub>	<sup>1</sup> A <sub>1</sub>	<sup>2</sup> A <sub>1</sub>	<sup>2</sup> B <sub>1</sub>	<sup>2</sup> A <sub>1</sub>	<sup>2</sup> B <sub>1</sub>
ρ <sub>b</sub> (E-N)	0.312	0.328	0.315	0.120	0.125	0.120		
∇ <sup>2</sup> ρ <sub>b</sub> (E-N)	-0.37	-0.72	-0.43	0.70	0.67	0.69		
ε(E-N)	0.22	0.25⊥	0.40	0.17⊥	0.27⊥	0.06⊥		
q(E)	1.06	1.42	1.22	1.51	2.06	1.69		

<sup>a</sup> See Table 5 and the methods section for an explanation of the calculated properties. <sup>b</sup> Calculated from Hartree-Fock wave functions using the 6-311G(d,p) basis at the HF/6-31G(d) geometry of the respective neutral.

negative Hartree-Fock orbital energy (9.5 eV) by more than 2.5 eV. However, the electron correlation correction is *not* larger than in the case of b<sub>1</sub> ionization (ca. 1 eV), and thus the final ΔPUMP4/6-31G(d) and ΔCCSD(T)/6-31G(d) ionization energies of 7.8 eV (which compare well with the experimental result for **1** with R = *tert*-butyl, Table 7) deviate from the prediction based on Koopmans' theorem by more than 1.5 eV. What is the nature of the strong relaxation of the wave function upon ionization of an electron from the a<sub>1</sub> orbital? Table 8 summarizes the relevant properties of the charge densities in **7** and **7<sup>+</sup>** (<sup>2</sup>A<sub>1</sub> and <sup>2</sup>B<sub>1</sub> states). On the background of the discussion of the neutral aminocarbenes (see section IV), π-electron delocalization is apparent in the properties of the <sup>2</sup>A<sub>1</sub> state of the carbene cation radical. Here, the carbene's C-N bond has its major axis *perpendicular* to the molecular plane. Moreover, both the covalent C-N bond order (as measured by ρ(r<sub>b</sub>)) and the degree of covalence in the C-N interaction (as measured by ∇<sup>2</sup>ρ(r<sub>b</sub>)) are larger in **7<sup>+</sup>** (<sup>2</sup>A<sub>1</sub>) than in neutral **7**. Despite the fact that in the neutral **7** the lone-pair a<sub>1</sub> orbital is almost entirely located on the carbenic carbon, only 36% of the positive charge are located on this atom. In contrast, the properties of the <sup>2</sup>B<sub>1</sub> state of **7<sup>+</sup>** resemble much more the situation in the neutral carbene (see Table 8).

We conclude that removal of an electron from the carbene lone-pair electron of a C=C unsaturated cyclocarbene of the imidazol-2-ylidene type increases the π-electron delocalization in the five-membered ring. The situation bears a certain similarity to protonation of **7** (see section VI and refs 10 and 11), where electron density is also removed from the vicinity of the divalent carbon atom with a concomitant increase of π-electron delocalization. This suggests that the nonbonding *in-plane* electron density at the carbene center interferes and reduces cyclic electron conjugation in **1** and **7**, thus lowering the importance of ylidic resonance structures in stable carbenes of the Arduengo type.<sup>10</sup>

For the corresponding silylene **13** these effects are less pronounced: Qualitatively, the calculated energies of the b<sub>1</sub> (HOMO) and a<sub>1</sub> orbitals yield the same ionization pattern as the ΔPUMP4 and ΔCCSD(T) calculations (see Table 7). Relaxation (ca. 1 eV) and electron correlation (ca. 1 eV) effects for the b<sub>1</sub> ionization are very similar to those found in the carbene case and show that this process is well described by the Koopmans approximation. The a<sub>1</sub> ionization is again subject to a larger relaxation of the wave function in the cation-radical (1.5 eV) but the correlation correction for this process is in the usual range of ca. 1 eV. Overall, the relaxation effect is not sufficiently large to reverse the ionization pattern predicted from the orbital energies, in contrast to the situation in the carbene analog **7**. This is also evident from the properties of the charge distributions (Table 8): While the <sup>2</sup>B<sub>1</sub> state of **13<sup>+</sup>** resembles closely the neutral silylene, there is a certain increase in the covalent Si-N interaction in the <sup>2</sup>A<sub>1</sub> state, but the changes in cyclic electron delocalization are less pronounced than in the

carbene case. This is most clearly recognized in the charge of the divalent atom, which increases by 0.55e upon removal of the a<sub>1</sub> electron from **13**, compared to 0.36e in **7**. Overall, it appears that, in contrast to the carbene, in cyclosilylene **13** Koopmans' theorem is valid for *both* lowest energy ionization processes because cyclic electron delocalization is less pronounced in the <sup>2</sup>A<sub>1</sub> state of the silylene cation-radical **13<sup>+</sup>** than in the corresponding carbene system **7<sup>+</sup>**.

## Summary

We have considered thermodynamic, magnetic, and structural criteria, the properties of the molecular charge densities, and low-energy ionization processes to evaluate the role of cyclic electron delocalization in imidazol-2-ylidenes and their silicon analogs. The following conclusions can be drawn from these different criteria: (1) Planar amino substituents stabilize singlet carbenes significantly and the presence of the C=C double bond in the cyclic imidazol-2-ylidene brings about an additional stabilization of ca. 25 kcal/mol. Slightly smaller but qualitatively similar effects are found in the isostructural silylenes. (2) Structural differences between C=C-unsaturated cyclocarbenes, their C-C-saturated analogs, and the corresponding saturated hydrocarbons are consistent with bond length compensation due to cyclic electron delocalization. The effects for the homologous silylenes are qualitatively similar but quantitatively smaller. (3) In contrast to the C-C-saturated imidazol-2-ylidene, the C=C-unsaturated imidazol-2-ylidene and the imidazolium cation are characterized by large anisotropies of their magnetic susceptibilities, which derive from magnetically induced currents through the interatomic surfaces of the ring atoms. The calculated anisotropies of the magnetic susceptibilities are ca. 60% of the value in benzene and can thus be taken as an indication for cyclic electron delocalization in these species. Similar effects, although to a smaller extent, characterize the corresponding cyclosilylenes. (4) Analysis of the charge densities, according to the "atoms-in-molecules" method, does not reflect p<sub>π</sub>-p<sub>π</sub> back-bonding in mono- and diamincarbenes and -silylenes, as anticipated by the resonance model. Rather, this model suggests that reorganization of the atomic basins and thus different degrees of electrostatic interactions and polarization of the nitrogen atoms are responsible for the large rotational barriers and the associated structural changes in these molecules. In light of the almost negligible reflection of conjugation in the noncyclic model systems, the topological analyses do provide evidence for some degree of cyclic electron delocalization in C=C-unsaturated Arduengo-type cyclocarbenes (and to a smaller extent in C=C-unsaturated cyclosilylenes) as compared to their C-C-saturated analogs. π-Electron delocalization increases significantly upon protonation of (di)aminocarbenes. (5) An unusually large relaxation of the wave function in terms of enhanced cyclic electron delocalization occurs upon removing an electron out of the carbene "lone pair" of imidazol-2-ylidene. A qualitatively similar but quantitatively smaller effect is found for the corresponding silicon analog. It appears that the presence of localized "in-plane" electron density at the divalent group 14 center prevents more extensive cyclic electron delocalization in C=C-unsaturated cyclocarbenes and -silylenes.

With the help of these results, the following general conclusions can be drawn: (i) Qualitatively, all criteria point to the occurrence of cyclic electron delocalization in the C=C-unsaturated carbenes of the imidazol-2-ylidene type **1**, in comparison to the corresponding C-C-saturated imidazol-2-ylidenes **2**. However, the "aromatic character" of these molecules is significantly smaller as compared to prototype aromatic systems such as imidazolium cations or benzene.

However, the different theoretical approaches lead to different conclusions regarding the degree of cyclic electron delocalization in these systems. The magnetic and thermodynamic criteria point to *significant* (even strong) conjugation in the C=C-unsaturated carbene and silylene, in agreement with the conclusions of the independent recent study by Böhme and Frenking.<sup>19</sup> On the other hand, the topological analyses point to a *small but still discernible* role of cyclic conjugation in these systems. Using orbital-based methods for the analysis of the charge densities in noncyclic and cyclic aminocarbenes,  $p_\pi$ - $p_\pi$  delocalization appears to be more pronounced.<sup>19</sup> The very different conclusion on conjugation in model aminocarbenes obtained with orbital-based methods is due to changes in the locations of the bond critical points of the topological analysis. Thus, different measures of the idea of aromaticity<sup>20</sup> provide different quantitative answers and therefore the question "To which degree are imidazol-2-ylidenes stabilized by cyclic electron delocalization?" can only be answered qualitatively. Large effects in the topological analysis of the charge densities are observed when electron density is removed from the vicinity of the carbenic carbon, e.g. upon protonation or ionization. According to this analysis, the low quantitative importance of cyclic electron delocalization in **1**, as reflected in the measured electron density distribution, the calculated Laplacian distributions for **7** as compared to **9**, and the small structural differences between C=C-unsaturated and -saturated cyclocarbenes, can be attributed to the role of the carbene in-plane lone pair as an "electronic barrier" to cyclic delocalization.

(ii) Cyclic electron delocalization is also apparent for the silicon analogs of imidazol-2-ylidenes **3**, although to a smaller extent than for the isostructural carbenes. Thus, the earlier conclusion that C=C-unsaturated cyclosilylenes of type **3** are "aromatic"<sup>6</sup> should be set in relation to the degree of electron delocalization in the isostructural carbenes.

**Acknowledgment.** The authors express their sincere gratitude to Prof. Richard F. W. Bader, McMaster University, for providing the results on the atomic contributions to the magnetic susceptibilities as well as for many stimulating discussions. We thank Dr. Anthony J. Arduengo III and Prof. Gernot Frenking for providing preprints of their recent work (refs 4 and 19) and many constructive suggestions. We are grateful to Dr. Graham A. McGibbon for helpful comments on the final version of the manuscript. C.H. acknowledges a Kekulé Ph.D. fellowship from the Fonds der Chemischen Industrie. T.M. is indebted to the Minerva Foundation for a postdoctoral fellowship. H.S. and Y.A. thank the Alexander von Humboldt Stiftung for a Max-Planck and a Lise Meitner Research award, respectively. Financial support by the Deutsche Forschungsgemeinschaft, the Fonds der Chemischen Industrie, the Volkswagen-Stiftung, and the US-Israel Binational Science Foundation is gratefully acknowledged.

JA9523294